

## Abstract

BREWER, ROGER ALAN. Electrical Energy Storage to Meet Evolving Aircraft Needs. (Under the direction of Dr.Subhashish Bhattacharya).

The value of “ultracapacitors” (also referred to as “supercapacitors” or “electric double layer capacitors” in some literature but hereafter largely referred to as ultracapacitors) as an augmentation device when placed in parallel with “electrochemical” energy storage (i.e. batteries) is presented in this paper as well as a peak power assist case where ultracapacitor technology is paralleled with a primary power supply. Since ultracapacitors possess unique attributes due to their higher energy storage density (or Joules/WattHrs per mass) compared to conventional capacitors while maintaining the peak power providing capability (to some degree) typical of conventional capacitors they may provide a near term solution in applications demanding longer battery operating life and power system robustness. Such demands may be more pronounced by the onset of evolving peak power loads and “cold-crank” Auxiliary Power Unit (APU) electric-starting in demanding cold temperature environments.

The potential benefits of an ultracapacitor in parallel with a battery will be illustrated through a very simple lab demonstration as well as a more complex system consisting of a large motor “outrush” load (cold-cranking condition) through the use of a computer simulation tool (Simulink). Similarly, a peak power case will be evaluated through a simple lab demonstration and computer modelling (LT Spice IV). All simulations and testing are intended to illustrate basic transient performance behavior as improved energy storage technology might be applied to a power system (versus steady-state or frequency response performance). In addition to the ultracapacitor discussions and demonstration, other forms of advanced energy storage will be reviewed for their potential near or long term application in meeting the evolving needs of aircraft. All results and discussions have been presented in a general nature and not intended to be targeted at any specific aircraft configuration. A section will also briefly discuss and explore literature relevant to more detailed aspects of modeling ultracapacitor devices.

Based on the outcome of the case studies a recommended and high level technology roadmap will be created for next generation ultracapacitor technology concepts that may contribute to further meeting the needs studied. The final summary section will include a list of captured items that would be prudent as follow-on activity and discuss parallels that are relevant beyond aircraft power systems to the DC Micro-grid. The final summary section will also reemphasize the differences learned in the two case studies and how these differences drive differing aspects of ultracapacitor technology roadmaps.

© Copyright 2014 by Roger Alan Brewer

All Rights Reserved

Electrical Energy Storage to Meet Evolving Aircraft Needs

by  
Roger Alan Brewer

A thesis submitted to the Graduate Faculty of  
North Carolina State University  
in partial fulfillment of the  
requirements for the Degree of  
Master of Science

Electrical Engineering

Raleigh, North Carolina

2014

APPROVED BY:

---

Dr. Aranya Chakraborty

---

Dr. Mesut Bran

---

Dr. Subhashish Bhattacharya  
Chair of Advisory Committee

## Biography

Roger Alan Brewer's life started in the state of Illinois in August 1965, the son of a carpenter. Wonderfully blessed with a loving family, he loved learning and exploring outside and being with family as a child and throughout the early years of his life up through high school. Baseball and baseball card collecting were among his favorite hobbies although he quickly realized the unique value and opportunities a great education could offer. As he continued to mature, he had always admired and respected one of the dear, close friends of his family Dr. Wayne Lichtenberger. Dr. Lichtenberger had graduated from the University of Illinois with his Undergraduate degree, Master's degree and his PhD in Electrical Engineering many years prior to Roger's childhood. Dr. Lichtenberger held a tremendous amount of respect within the Electrical Engineering community, both at Illinois and also at the University of California-Berkeley and the University of Hawaii where he subsequently held teaching and research positions after leaving Illinois.

As Roger graduated high school, his earlier childhood dream of becoming a professional baseball player continued to give way to what was becoming what he considered a more realistic but yet highly noble and honorable vision of becoming an Electrical Engineer. Finally, after four years of study at the University of Illinois preceded by two years of prerequisite courses at a local Junior College, he completed his Bachelor of Science Degree in Electrical Engineering in 1989.

Now eager to begin his professional career in the engineering world and earn a much needed steady salary, Roger entered the workforce. Months of being a working, Electrical Engineer quickly became years and were accompanied by the joys of marriage, raising children and a career filled with mostly ups but some downs. Roger realized it was time to return to his passion of academics convinced of its unparalleled value. After many encounters in the working world there was no doubt in his mind those with more education were, at least in many cases, more satisfied with fulfilling and challenging work.

Upon being accepted at North Carolina State University, Roger embarked on a new journey. This journey would prove to be a challenging one as he struggled to balance work, family and school. However, with the tremendous support of family and many prayers he is reaching the end of his graduate school journey but with the striking realization he would not trade the journey struggle of these past years.

## Acknowledgements

Some of the research in this paper was made possible by funding under the F-35 JSRI EAU Inter-Work Transfer Agreement (IWTA) #14467 with the lab demonstration (for Battery Cold-Start assist evaluations) made possible under C-5 Systems Improvements Project Id 414-D1-540 funds.

I would like to thank the Evans Capacitor (Mr. Dave Evans), JSR Micro (Mr. Jeff Myron) and Qynergy (Dr. Viswanath Krishnamoorthy) companies and Mr. David Findley (Lockheed Martin Aeronautical Systems) for approval in sharing their technology summaries and key technical inputs. I would also like to thank Mr. Art Schuetze and Mr. Lee Jenderko, my colleagues at Lockheed Martin Aeronautical Systems-Fort Worth Texas, for key contributions and input in the ultracapacitor peak load testing and their many other technical contributions over these past years. I have learned immensely from both of these colleagues during my career at Lockheed Martin. I would also like to extend thanks to my Senior Manager at Lockheed Martin, Hal Morrison, for his review of my initial data for public release suitability as well as, again, Mr. Schuetze and Curt Chankaya (again with Lockheed Martin). I thank the Lockheed Martin Aeronautical Systems-Marietta Georgia Flight Line Electronics Lab, specifically Roger Somerville, for the exceptional and timely support of the lithium-ion ultracapacitor testing (with the Nickel Cadmium cell) under demanding other time constraints at the time of test.

I extend my special gratitude to Dr. Subhashish Bhattacharya at North Carolina State University for overseeing my work, for without his oversight and assistance none of this would have been possible. I extend my thanks to both Dr. Mesut Baran and Dr. Aranya Chakraborty, also both at North Carolina State University, for agreeing to co-chair my Thesis and their flexibility in attending my final oral defense.

Last, but certainly not least, I would like to thank my beautiful wife Stenelle Brewer and my daughter Sarah Brewer for their unwavering support throughout my entire graduate program and for helping me to overcome my own personal challenges during a period of transition in all of our lives. I also thank both of my dogs, Kiwii and Crème Brule, for their excitement and enthusiasm on all those jogs where I needed to air out my mind from a long afternoon of studying. I love you all! I thank God for allowing his Spirit to be with me and carrying me through all the times and trials of my life.

# Table of Contents

List of Tables .....	v
List of Figures .....	vi
List of Symbols .....	vii
List of Symbols (Cont.) .....	viii
Chapter 1: General System Considerations and Discussion .....	1
1.1 Other Advanced System Considerations .....	2
Chapter 2: Capacitor Technology .....	4
2.1 Modelling UltraCapacitor Devices Literature Survey .....	7
2.2 Technology Comparisons .....	8
2.2.1 Electric Double Layer (Ultracapacitors) .....	11
2.2.2 Hybrid “asymmetric” Ultracapacitors .....	12
2.2.3 Lithium ion Ultracapacitors .....	14
2.2.4 Hybrid Tantalum capacitors .....	15
Chapter 3: Application Studies .....	16
3.1 Application #1 - Simulation of Ultracapacitor in Parallel with Battery .....	16
3.1.1 Overview .....	16
3.1.2 Simulation Results .....	20
3.1.3 Simulation Conclusion .....	23
3.1.4 Lab Demonstration .....	24
3.1.5 Technology Roadmap for Ultracapacitor as Electric-Start Assist Device .....	26
3.2 Application Study #2 – Peak Load Assist with Capacitance .....	26
3.2.1 Overview .....	26
3.2.2 Simulation .....	27
3.2.3 Simulation Conclusion .....	29
3.2.4 Lab Testing .....	30
3.2.5 Technology Roadmap for Peak Load Assist - Ultracap as a Baseline .....	32
Chapter 4: Summary .....	33
4.1 Follow-On Activity .....	35
References .....	37
References (Cont.) .....	38
Appendix .....	39
Appendix A- Generator Instability in Aircraft Power .....	40

## List of Tables

Table 2-1: Capacitor Technology Comparison .....	11
Table 3-1: Boost Capacitance characteristics for Simulation.....	19
Table 3-2: Battery Assist Simulation Results.....	20
Table 3-3: System Voltage Comparisons for Battery Start Assist .....	23
Table 3-3 (Cont.): System Voltage Comparisons for Battery Start Assist .....	24
Table 3-4: Ultracapacitor Technology Resistance Comparisons.....	33
Table 4-1: Energy Storage Investment Strategy Proposal.....	35

## List of Figures

Figure 1-1: Energy Storage Throughout the Applications.....	1
Figure 1-1 (Cont.): Energy Storage Throughout the Applications.....	2
Figure 1-2: Aircraft APU Electric-Start Characteristic .....	2
Figure 1-3: Weapon Rapid Turn-on Profile .....	3
Figure 1-4: Hybrid Vehicle Parallels.....	3
Figure 2-1: Parallel Plate Capacitor .....	6
Figure 2-2: Electric Double Layer Capacitor Structure.....	6
Figure 2-3: Energy and Power Relationships .....	7
Figure 2-4: Electrical Circuit Models of Ultracapacitors .....	8
Figure 2-5: Energy Storage Ragone Plot.....	9
Figure 2-6: Energy Storage Ragone Plot (expanded).....	10
Figure 2-7: Electric Double Layer Anatomy .....	12
Figure 2-8: QynCap Anatomy .....	13
Figure 2-9: Hybrid Cell Characteristics .....	13
Figure 2-10: QynCap Cell Structure and Prototype .....	14
Figure 2-11: Lithium Ion Capacitor Characteristics.....	14
Figure 2-12: Hybrid Tantalum Cell .....	15
Figure 2-13: Hybrid Tantalum Package .....	16
Figure 3-1: Ultracapacitor in parallel with Battery Simulation Circuit.....	17
Figure 3-2: Simulation Results (Battery Voltage).....	21
Figure 3-3: Simulation Results (Battery Peak Current).....	22
Figure 3-4: Lithium Ion Supercapacitor Test Cell.....	25
Figure 3-5: Battery voltage “sag” tests (Before and after LIC in parallel).....	26
Figure 3-6: Peak Load Buffering LT Spice IV Simulation Circuit .....	27
Figure 3-7: LT Spice IV Simulation Results - 30 $\mu$ F Low Boost Capacitance with Constant Power Load.....	28
Figure 3-8: LT Spice IV Simulation Results – 2.9F Boost Capacitance with Constant Power Load ..	29
Figure 3-9: Step Load Initial Test Layout Concept.....	30
Figure 3-10: Step Load Testing with 40-amp load.....	31
Figure 3-11: Step Load Testing with 200-amp load.....	32
Figure A-1: Generator Stability Study Model .....	41
Figure A-2: Generator Stability Study Results.....	43



## List of Symbols

awg	Gage
AWG	Gage
A	≡Area
AHr	Amp Hours
AC	Alternating Current
APU	Auxiliary Power Unit
BoostCap	Boost Capacitance
C	degrees Celsius
C	≡Capacitance
d	≡distance between capacitor plates
DC	Direct Current
DOD	Depth of Discharge
$\epsilon$	≡permittivity
emf	electromotive force
esl	equivalent series inductance
esr	equivalent series resistance
E	≡Electric Field strength
EDLC	Electric Double Layer Capacitor
EESU	Electrical-Energy-Storage-Unit
fGMC	femto Giant Magneto Capacitance
F	Farad, Farads
F	degrees Fahrenheit
H	Hydrogen
Hz	Hertz
I	≡Current
JSRI	Joint Strategic Research Initiative
k	kilo
kg	kilograms
kW	kilo Watts
LIC	Lithium Ion Supercapacitor
Li Ion	Lithium Ion
m	milli
M	Mega

## List of Symbols (Cont.)

Ni	Nickel
O	Oxygen
P	≡Power
PCB	Printed Circuit Board
PHC	preceramic polymer poly (hydridocarbyne)
PWB	Printed Wiring Board
sec	seconds
secs	seconds
SOC	State of Charge
Ta	Tantalum
U	≡Stored Energy
V	Volts
VAC	Volts Alternating Current
VDC	Volts Direct Current
W	Watts
Whr	Watt Hours
Whrs	Watt Hours
WHRS	Watt Hours

# Chapter 1: General System Considerations and Discussion

In applications where large transient electrical loading demands are placed on electrochemical batteries traditionally used in military vehicles such as modern aircraft, ground vehicles and other platforms, batteries experience a high degree of induced stress. Specifically, the stress a battery might experience is pronounced under conditions where vehicles may be operating under extreme temperature conditions, such as providing “cold-cranking” power to a starter motor at the onset of startup. Since electrochemical batteries store and deliver power involving chemical reactions (versus “electrostatically” as in the case of capacitors) a tremendous amount of internal heating with electrode material expansion and contraction results throughout a complete charge/discharge cycle (Reference 1).

As the chemically based constraints are coupled with the higher resistance associated with the liquid based battery electrolytes (with resistance inversely proportional to temperature), a high induced stress mechanism is established. Experience in the

field has indeed shown that battery maintenance intervals (and potential battery replacement) on the order of 120 day cycles are possible for military aircraft and perhaps even shorter for high end use commercial airliners. In cases where a minimum voltage must be maintained to a starter motor, a battery system may also need to be oversized (more cells in series) to meet voltage capability requirements and/or oversized to handle the peak power required. Batteries alone may not be optimum to meet these requirements with some varieties more inefficient in terms of peak power delivery.

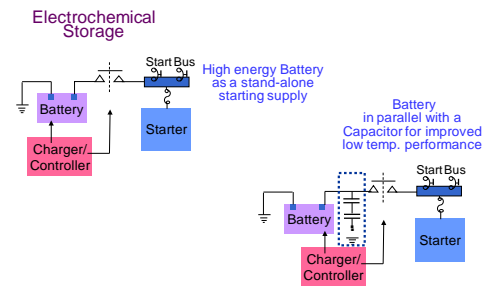


Figure 1-1: Energy Storage Throughout the Applications

Figure 1-1 to the right and below illustrates concepts involving various forms of energy storage utilization in system design. The decaying exponential characteristics of a typical aircraft Auxiliary Power Unit (APU) Starter Motor is also provided in figure 1-2 below although not specific to any configuration.

## Electric Double Layer Storage

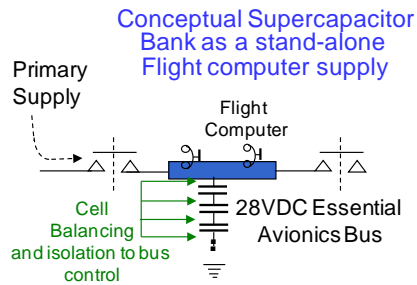
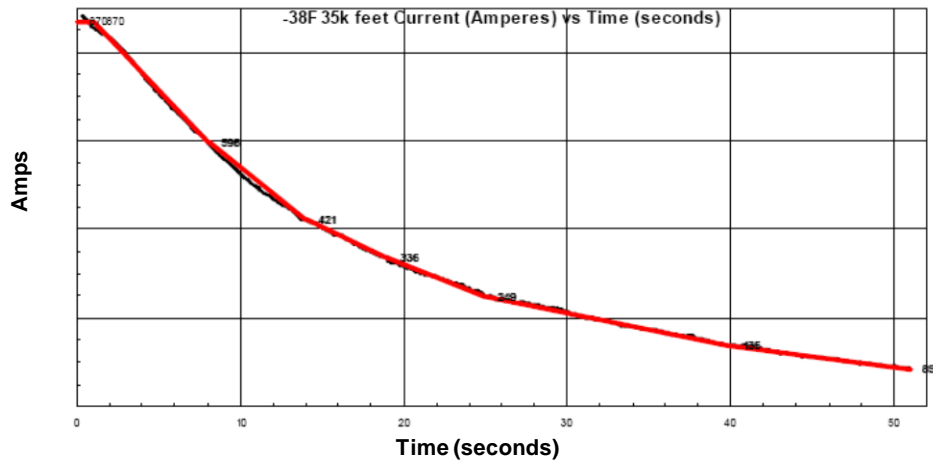


Figure 1-1 (Cont.): Energy Storage Throughout the Applications



... 3 of these attempts allowed in a 5 minute period

Figure 1-2: Aircraft APU Electric-Start Characteristic

### 1.1 Other Advanced System Considerations

In addition to the potential system applications involving electric-start assist, other advanced applications for future aircraft may include needs for a tremendous amount of peak power to support rapid turn-on loads where typical generator (or possibly even more likely the driving turbine) response time may be inadequate. Figure 1-3 below provides a hypothetical power profile for such a load.

Other applications may involve the ability to “sink” large amounts of “back-emf” (or regenerative energy, i.e. “regen”) and potentially use the regen as a recharge source to optimize overall vehicle efficiency. A comparison to such issues being explored and matured in the hybrid vehicle industry is provided in Figure 1-4.

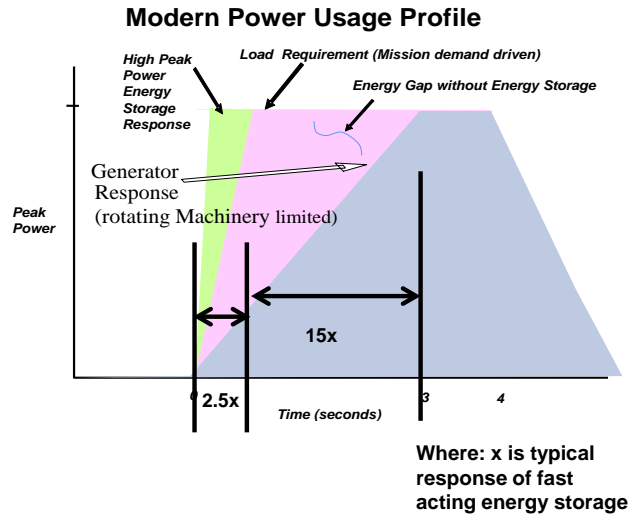


Figure 1-3: Weapon Rapid Turn-on Profile

• **More Electric Vehicle challenges are not unlike those of the Hybrid Vehicle industry**

- High levels of regenerative energy during vehicle braking parallels flight control motor braking although ...
  - Energy levels differ
- Recaptured energy allows Hybrid Vehicle to propel without Internal Combustion Engine
- Hybrid and More Electric Aircraft architectures are driving specific energy and power density improvements of energy storage components

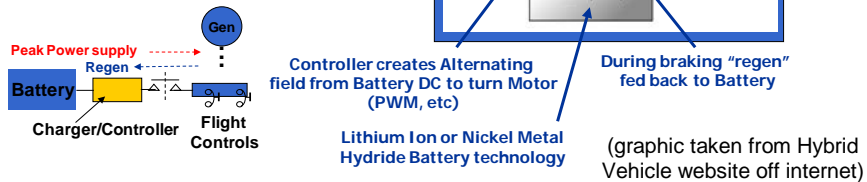


Figure 1-4: Hybrid Vehicle Parallels

In summary, many of the key aspects that are researched in any energy storage technology for evolving or existing applications can be summarized as follows:

- High energy density (kJoules per pound and per in<sup>3</sup>)
- High peak power density (kWatts per pound and per in<sup>3</sup>) or even more appropriately low equivalent series resistance with a target of: high  $v_{cell}$  rating/esr ratio
- Safety (no hazardous material “outgassing” on overcharge)
- Charge/discharge efficiency (minimal loss between charge/discharge as waste heat)
- Regenerative energy absorption (ability to absorb regen without degradation, outgassing, etc.)
- Packaging robustness (does the packaging approach optimize peak power performance, minimize voids and maintain thermal integrity)
- Aircraft environment (survive thermal, vibration, humidity)
- Technology maturity (can the technology be readily fielded if required or are there significant technology hurdles)
- Total Cost (\$/kWhr and \$/kW)
- Could the technology be a “game changer?”

## Chapter 2: Capacitor Technology

With an overview of the system needs for energy storage established it is appropriate to review the foundational equations governing energy storage and explore how this is applied to the approaches being undertaken by the various developers in the field.

The equation governing the amount of stored energy that can be achieved in any capacitor technology (or “electrostatic” device) is as follows (with  $U$ =stored energy,  $V$ =Capacitor Breakdown Voltage and  $C$ =Capacitance):

$$(2.1) \quad U = 1/2 * C * V^2$$

Where:

$$(2.2) \quad C = \epsilon * A / d$$

With:  $A$ =Area of the capacitor plates

$d$ =distance between the capacitor plates

$\epsilon$  = relative permittivity of the dielectric  $\epsilon_r$  x permittivity of free space  $\epsilon_0$   
 ( $\epsilon_0=8.85418782 \times 10^{-12}$  Farads/meter) and where  $\epsilon_0$  is also defined as  $\epsilon_0=1/\mu_0 c^2$  ( $c$ =speed of light in a classical vacuum and  $\mu_0$  is defined as the magnetic constant or  $4\pi \times 10^{-7}$ )

In Equation (2.1) above, the expression for stored energy has been derived from the work performed to establish the Electric Field "E" across the parallel plate structure shown in figure 2-1. Work, defined as the total to assemble stored charges, can be written in the integral form for distributed

charges as follows:

$$(2.3) \quad U = 1/2 \int \rho_v V dv$$

Using relations:  $\rho_v = \nabla \cdot \mathbf{D}$  and  $E = -\nabla V$  it can be shown that:

$$(2.4) \quad U = 1/2 \int \epsilon^* E^2 dv = 1/2 \epsilon^* E^2 Ad = (1/2 \epsilon^* V^2 A)/d = 1/2 C V^2$$

In arriving at Equation (2.4) above from Equation (2.3), Maxwell's equation in point form has been applied or: (2.5)  $\rho = \nabla \cdot \mathbf{D} = Q = \epsilon^* E \cdot \mathbf{A}$  (where the divergence theorem has been applied to the electric flux density D) along with the substitution: (2.6)  $V = - \int E \cdot dl = -Ed$  (from the definition of electric potential across distance "d" derived from Coulomb's Law with the potential difference defined as the amount of work to move a unit charge from A-B or  $V_{A-B} = W_{A-B}/Q$ ). Finally, total Stored Energy becomes:

$U = 1/2 \int \epsilon^* E \cdot \mathbf{A} \cdot (-Ed) = 1/2 \epsilon^* E^2 Ad$  from substituting (2.5) and (2.6) above, integration across the plate distance d and pulling out the constant terms  $\epsilon$ , E and A.

In Equation (2.2) above, the expression for basic capacitance  $C=Q/V$  is combined from Gauss's Law to arrive at:

$$(2.7) \quad Q = \epsilon^* E \cdot \mathbf{A}$$

with the Electric Field defined as normal to the Gaussian surface of a parallel plate with ds (differential surface area element) also normal to the same surface (dot product or cosine of angle between the two =1). Field fringing has been neglected in deriving this equation

(See Reference 8 for above equation and discussion)

Figure 2-1 below defines the Gaussian surface (in blue) across a conventional parallel plate structure used to derive Equation (2.7) and the Electric Field “E” to establish Equation (2.6) above.

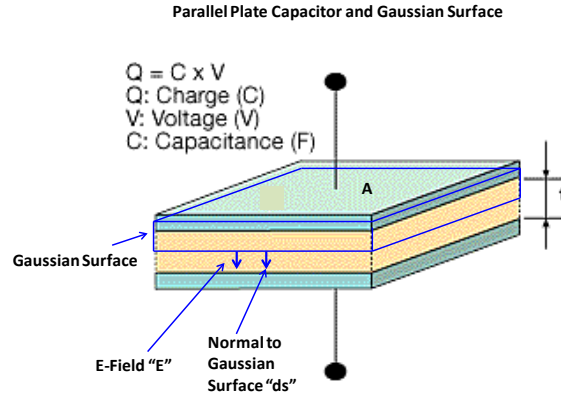


Figure 2-1: Parallel Plate Capacitor

From Equations (2.1) and (2.2) it can be seen that to maximize the amount of stored energy (also proportional to capacitance) “A” must increase while “d” must decrease. This is the essential element of ultracapacitor design where an extremely small separation distance “d” (at the atomic level) is achieved with highly porous carbon electrodes to achieve high “A” as compared to traditional capacitors.

Figure 2-2 below provides a typical cross-sectional view of an ultracapacitor (taken from Reference 5) where the basic electric double layer structure separating the positive and negative charges in principle corresponds to the parallel plate structure shown in figure 2-1 above.

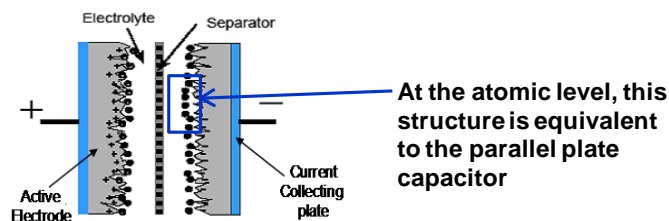


Figure 2-2: Electric Double Layer Capacitor Structure



Other capacitor innovations involve increasing V to impact a higher stored energy “U” although, as will be shown in the “Technology Comparison” Section below, with less success.

A summary of the discussion above with relevant relationships is provided in Figure 2-3 below.

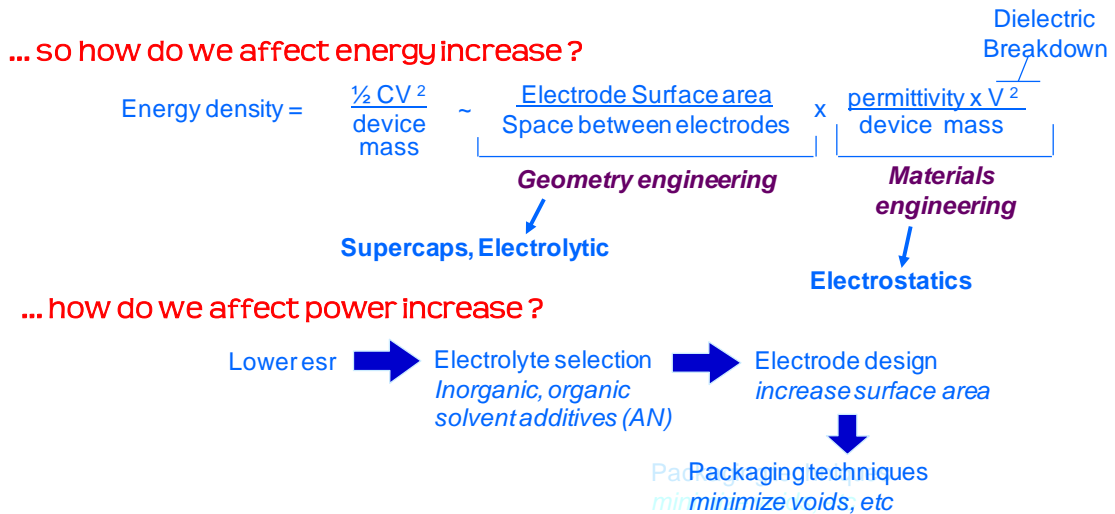
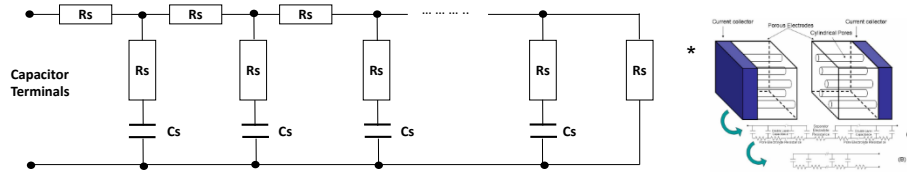


Figure 2-3: Energy and Power Relationships

## 2.1 Modelling UltraCapacitor Devices Literature Survey

Various literature exists discussing detailed and equivalent circuit models of ultracapacitor technology. One such paper (Reference 11) highlights the nonlinear effects (in relation to operating voltage) and RC time constant nature of ultracapacitors for a truly representative circuit model. More specifically, ultracapacitors have been described most completely as an RC ladder network (or transmission line model) in various literature including References 12 and 13. This effect has been discussed as related to the highly porous structure of the electrodes and heavily influenced by the charge transport process and groupings represented by an equivalent pore electrolyte resistance and interfacial double layer capacitance. Figure 2-4 illustrates the RC transmission line model given in the literature.



\*Porous electrode and RC ladder network model from Reference 13

Figure 2-4: Electrical Circuit Models of Ultracapacitors

Further work in the area of modeling more detailed voltage dependent non-linear effects of ultracapacitors in the application studies has been highlighted in the Follow-On Activity (Chapter 4.1) although modeling the BoostCap as a basic RC ladder network component was successful and compared very closely to the results demonstrated in Application #1 (Chapter 3.1) where the BoostCap was represented as a basic series/capacitor element in Simulink.

## 2.2 Technology Comparisons

While no one technology may simultaneously meet many of the desired characteristics for a given application, certain technologies when reviewed on a case by case basis might be considered more optimum than others.

When selecting a technology, as has been pointed out in energy storage conferences and related electrochemical capacitor papers (References 3 and 6), energy and peak power density terms should be considered highly dependent on rate of charge/discharge and temperature. Therefore, in referring to these “density” terms and the general values published from vendors, attention is required. Technologies driven by achieving higher “V” (as mentioned in the previous section) do tend to

achieve much higher power density since instantaneous power is dominated by  $P=I*V$  (current \* voltage). As was also shown in the presentation by Dr. John Miller (Reference 6) and others, measuring and ascertaining peak power density for any technology is highly dependent on the particular method used (i.e. “matched load” response) with energy density also influenced by other factors including temperature and discharge rate.

Given the above considerations, the “Ragone” chart in figure 2-5 below provides side by side published specific power and energy densities for various technologies. Where peak power and high voltage is required, ceramic capacitors, film capacitors, hybrid tantalums and other material

development technologies seeking improved breakdown voltage (as given in Equation (2.4)) may be optimal. Conversely, a higher level of energy storage for lower voltage applications may be optimally derived from electric double layer capacitors (or supercapacitors). Finally, higher energy can be obtained from battery (electrochemical) storage although, as shown in the expanded view in figure 2-6, some battery technologies appear to be successfully expanding peak power capability. Not included in the figures are impacts associated with cell monitoring electronics and conditioning and is a low to moderate impact for primarily lithium-ion and nickel-cadmium batteries. Fuel Cells (if they are indeed considered a form of “energy storage”), which rely on a continuous fuel supply (an oxidant), can achieve very high levels of energy density.

Far less mature technology development is seeking orders of magnitude increases in both peak power and energy such as Magnetic Capacitors and Metal-Air Batteries as shown in figure 2-5.

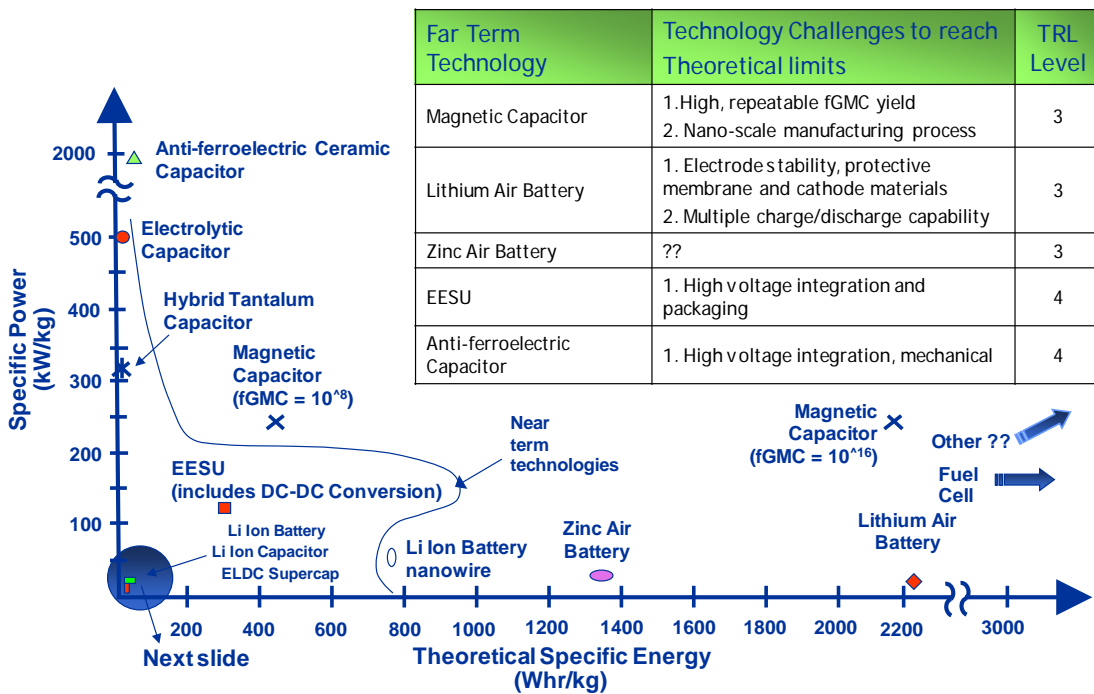


Figure 2-5: Energy Storage Ragone Plot

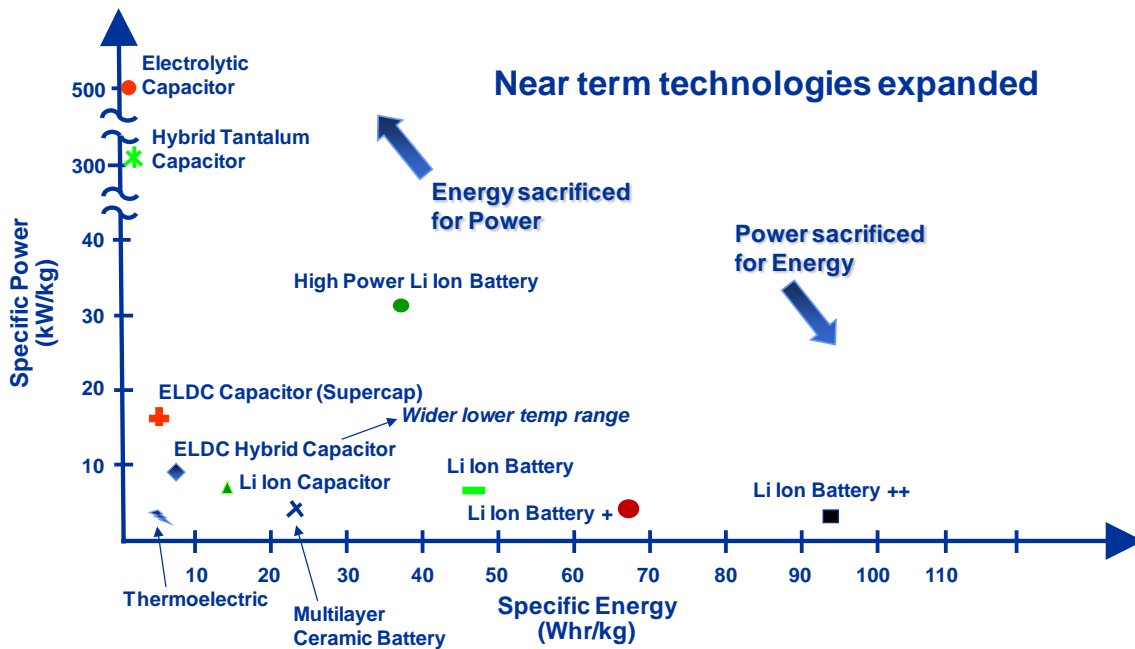


Figure 2-6: Energy Storage Ragone Plot (expanded)

Table 2-1 below provides another comparative breakdown among capacitor technologies and includes frequency and temperature capability as an additional attribute for comparison. In general, due to the larger time constant associated with “shuttling” charges across the porous structure of ultracapacitors, their time constant and thus associated frequency response is poorer. Also, most capacitors take temperature capability hits due to either their: a) associated grown oxide material (in the case of electrolytic and hybrid tantalums), b) thermal fatigue characteristics (in the case of a ceramic capacitor surface board mounted design) or c) liquid based electrolyte (in the case of the ultracapacitor technology). In general, it can also be stated any capacitor utilizing a grown oxide as its dielectric medium is limited in temperature capability due to oxide leakage at elevated temperature. Many of these comparisons came with input from capacitor developers (reference Acknowledgements section).

Table 2-1: Capacitor Technology Comparison

Technology	Temperature Capability	Voltage Capability	Energy Density	Power Density	High Frequency
Electrostatic	+ Moderate. Limited by thermal mismatch to PWB for surface mountable	++ Highest voltage per cell. Fewer cell stacking concerns for higher voltage applications	- Poor. Limited traditionally by electrode surface area	+ Good. Low esr, no electrolyte contributors	+ Good. High stability, low esr and esl. Not limited by high surface area of ELDC or electrolytes
Electrolytic	+ Moderate. Limited by leakage in dielectric material and electrolyte used	+ High voltage per cell. Fewer cell stacking concerns for higher voltage applications	+ Moderate. Improved surface area due to "anodically" formed oxide region	- Poor. Electrolyte/oxide contributes traditionally to "lossier" device	- Poorer. Traditionally lower stability, higher esr
Hybrid Tantalum	+ Moderate. Limited by leakage in dielectric material used	+ High voltage per cell. Fewer cell stacking concerns for higher voltage applications	+ Moderate. Contribution of electrochemical based cathode improves overall capability compared to Electrolytic/ Electrostatic	+ Good. High voltage dielectric anode improves capability as series cells reduced	- Poorer. Some higher esr contribution likely from electrolyte used
EDLC	- Poor. Limited by liquid electrolyte & leakage in dielectric material	- Low voltage per cell. Cell stacking and cell balancing concerns for higher voltage applications	++ Best. Atomic level dielectric "d" and porous carbon electrode dramatically increases	+ Good. Improvements in electrolytes drive up capability but can be limited by lossier electrolytes	-- Poorest. Less capable than even electrolytics with comparatively longer time constant

An overview (although not exhaustive) of some specific later generation capacitor technologies is now provided.

### 2.2.1 Electric Double Layer (Ultracapacitors)

Electric Double Layer ultracapacitors make use of two layers of separated charge at the atomic level (by a distance "d") to accomplish a high capacitance according to the equation that relates charge storage capability inversely to the distance "d" between two parallel plates. Additionally, ultracapacitors utilize two "symmetric" porous electrodes to increase the effective surface area between the separated charge plates further increasing available energy storage capability (according to the direct relationship between surface area and charge storage capability).

A liquid electrolyte, or mobilizing medium for ions, is contained within the capacitor structure and is

typically either organic or aqueous. Organic electrolytes typically allow for higher breakdown capability (voltage per cell 2.3V-2.8V) at the sacrifice of: a) safety (lower flash point temperature), b) low temperature capability and c) higher resistance. Aqueous electrolytes sacrifice the higher breakdown capability (voltage per cell ~ 1.23V) but with improved safety, low temperature performance and reduced resistance.

An inherent disadvantage associated with most traditional ultracapacitors is their low voltage capability per cell. This is a result of the small atomic scale separation distance “d” described above. Specifically, the benefits of grown dielectrics associated with traditional electrolytic capacitors (providing increased voltage capability per cell) or high dielectric ceramics is not achieved with ultracapacitor technology. Other advantages distinct to traditional capacitors are maintained with ultracapacitor technology, such as fast recharge/discharge rate, high efficiency (little lost energy throughout the charge/discharge cycle), high power density (kW/kg) and improved low/high temperature performance capability as compared to some battery technologies. Power densities on the order of 18kW/kg and energy densities on the order of 5Wh/kg or more are predicted for the symmetric technologies among the various developers. Figure 2-7 below provides a top level illustration of the Electric Double Layer concept and anatomy (taken from Reference 13).

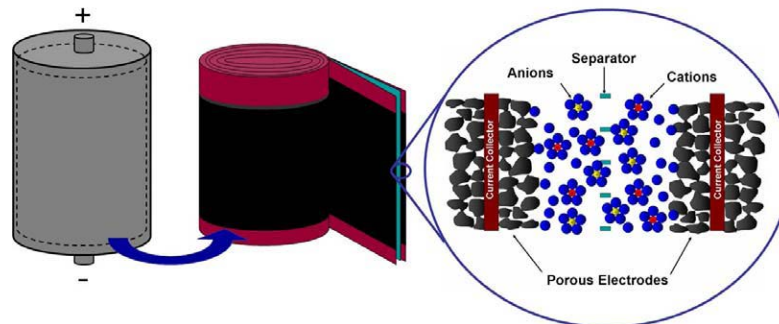


Figure 2-7: Electric Double Layer Anatomy

### 2.2.2 Hybrid “asymmetric” Ultracapacitors

The principle behind hybrid, or “asymmetric” ultracapacitors, includes the integration of a more traditional ultracapacitor (electric double layer type) electrode with a “battery-like” electrode structured into a single cell. Such a concept seeks to maintain the high power (kW) density and other benefits

associated with symmetrical ultracapacitors while improving energy (Whrs) providing benefits into a single device.

One such concept, the QynCap cell of Qynergy as shown in figure 2-8 below, makes use of a NiOH<sub>2</sub> (higher energy providing cathode) based battery electrode and a traditional Double Layer activated Carbon Capacitor (higher peak power providing anode) electrode. Power densities on the order of 1-10kW/kg and energy densities on the order of 5 – 10 Wh/kg are predicted for the QynCap cell. An aqueous electrolyte is used to improve low temperature performance.

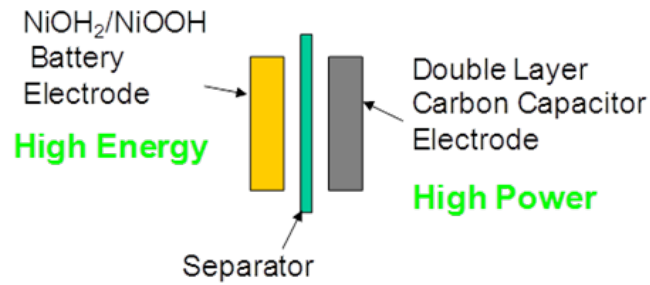


Figure 2-8: QynCap Anatomy

An additional illustration providing insight into the energy extraction benefits of the QynCap cell is provided in figure 2-9 below. As can be seen, since the battery electrode (electrochemical based cathode) voltage changes very little in comparison to the capacitor electrode (anode) voltage during discharge, a higher overall charge can be extracted since voltage differential change (or “U” in Equation (2.1)) is larger.

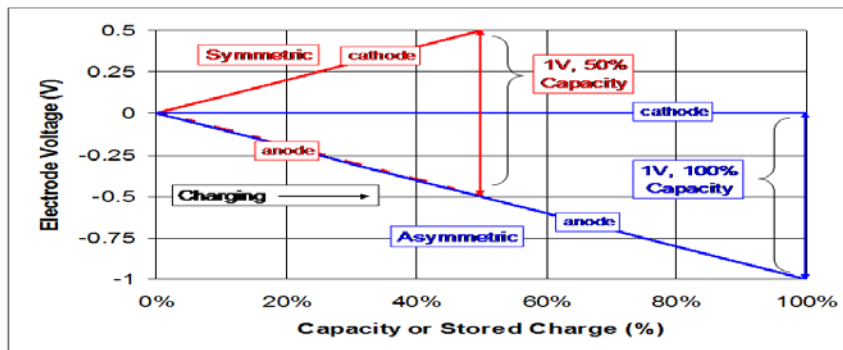


Figure 2-9: Hybrid Cell Characteristics

Figure 2-10 below provides a cutaway illustration view of a typical QynCap cell as well as a prototype QynCap cell.

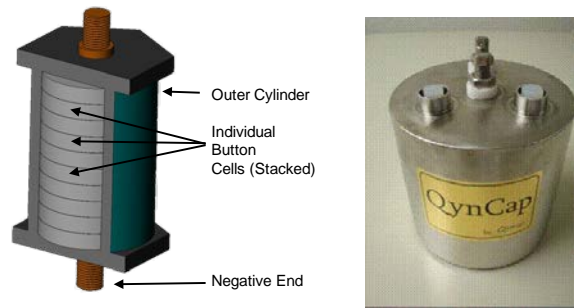


Figure 2-10: QynCap Cell Structure and Prototype

### 2.2.3 Lithium ion Ultracapacitors

The Lithium Ion Capacitor (LIC) can be considered another form of an “asymmetric” ultracapacitor. Lithium is used as a dopant on one of the electrodes (anode) with the cathode electrode similar in nature to a typical symmetric ultracapacitor consisting of activated carbon. The doping on the structure’s anode electrode has the effect of lowering its potential (in relation to the cathode) resulting in an overall higher voltage per cell device (see figure 2-11 below) resulting in higher “U” (see Equation (2.1)).

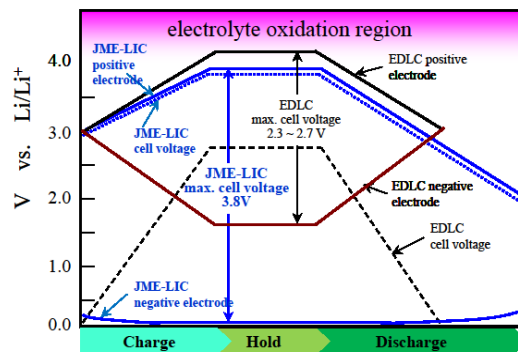


Figure 2-11: Lithium Ion Capacitor Characteristics



The combined affect is a device with improved energy density, self-discharge and voltage per cell capability over conventional “symmetric” ultracapacitors while also improving (or at least competitive with) the power density (kW/kg) offered from batteries. Other benefits of conventional capacitor technology might conceivably be retained with the lithium ion capacitor including robust charge/discharge C-rates and high temperature operation capability.

The typical energy density of LIC cells are currently 12Whr/kg with a cell voltage of 3.8V nominal. Dramatic reduction (70%) of DC-IR in the Gen 2 cells have improved efficiency at high currents and cold temperature performance. Gen3 cells will have much improved energy density.

### 2.2.4 Hybrid Tantalum capacitors

The hybrid tantalum capacitor approach, developed by Evans Capacitor, makes use of an electrochemical type electrode for the cathode and a tantalum anode formed dielectric ( $Ta_2O_5$ ) for enhanced voltage withstanding capability.

With the hybrid tantalum technology (as shown in figure 2-12 below) a large portion of the voltage potential across the capacitor structure is dropped across the more robust anode formed dielectric with enhanced stored charge capability provided at the “electrochemical like” cathode surface. Charge balance is maintained across the entire structure.

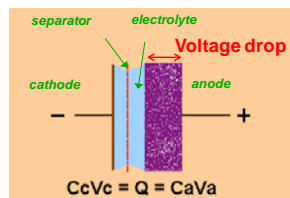


Figure 2-12: Hybrid Tantalum Cell

Another aspect of the Evans tantalum hybrid device is related to the packaging approach. A thin, flat package tends to minimize electrical resistance while maximizing heat dissipation (and surface area) thereby increasing the device’s peak power capability. The hybrid capacitor package is shown in figure 2-13 below.

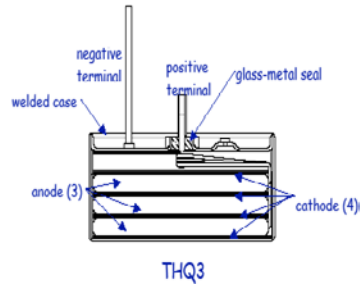


Figure 2-13: Hybrid Tantalum Package

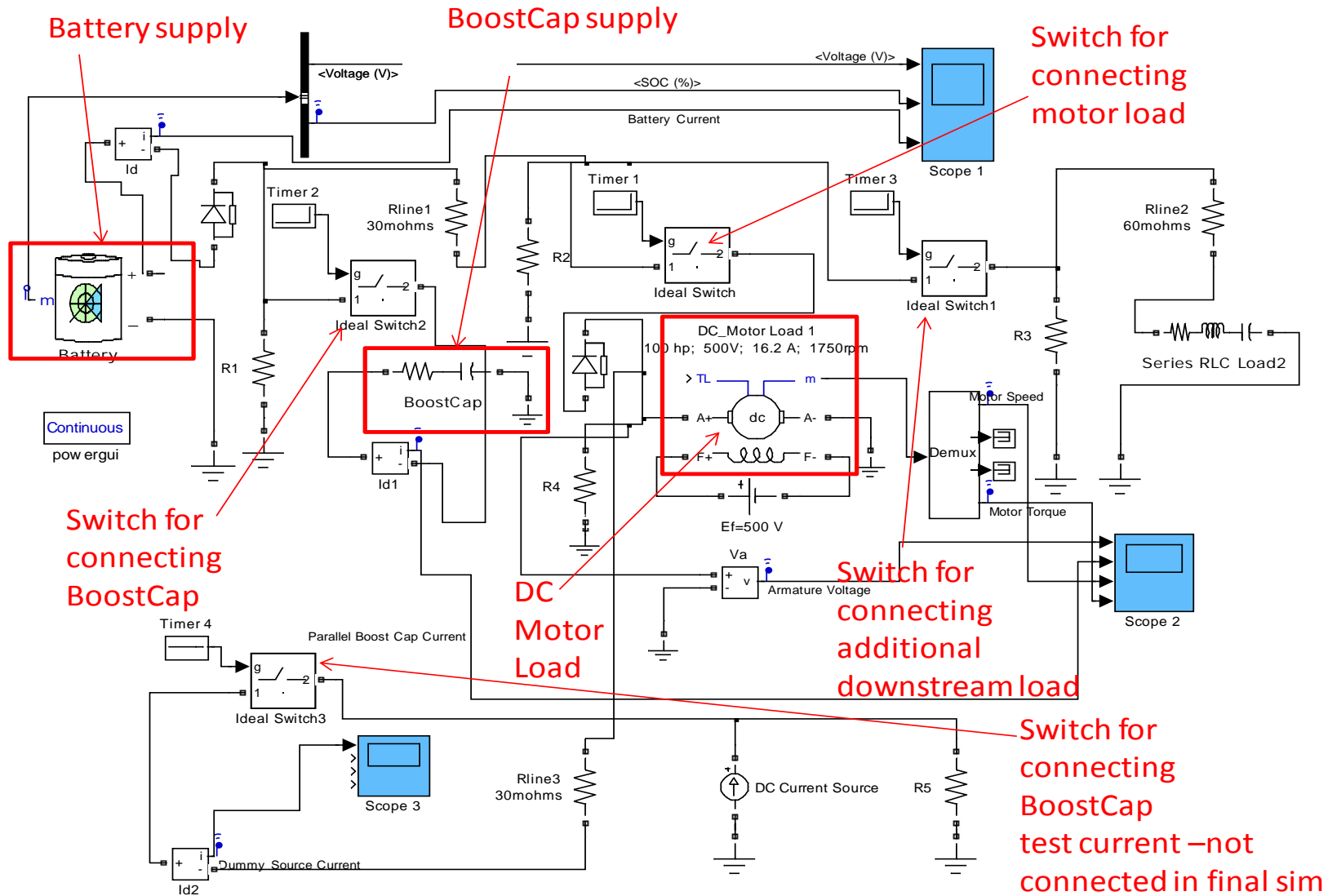
As with the other forms of hybrid capacitors, the technology seeks to combine both higher voltage per cell and power capability with some degree of higher energy storage capability. While the projected energy targets of this technology ( $< 5 \text{ Whr/kg}$ ) do not rival that of ultracapacitors, there are strong indications its specific energy surpasses that of conventional electrolytic or ceramic capacitors with similar frequency response and may be useful in certain pulse power applications.

## Chapter 3: Application Studies

### 3.1 Application #1 - Simulation of Ultracapacitor in Parallel with Battery

#### 3.1.1 Overview

Simulink (Sim Power Systems toolset) was used as the demonstration tool to explore the potential benefits of varying capacitance values (hereafter referred to as “BoostCap”) in parallel with a battery and connected to a motor load on startup through a switch. The simulation circuit is provided below.



Built in tools available with the standard Sim Power Systems package were utilized in developing the model, such as a Nickel Metal Hydride Battery and built in capacitor components. Resistances were included in series with each of the primary components, specifically a resistance was included in series with the BoostCap to model the capacitor's packaging and internal resistance with variations noted through the simulation.

A 220V nominal battery voltage was assumed to start a 100 horsepower DC Motor as well as a resistance in series with the Battery to simulate packaging resistance (approximated as 100 mohms).

In modeling the BoostCap, a 3,000 F single cell ultracapacitor was initially assumed (typical of a product available from Maxwell). Since a nominal 220V was to be obtained to match the battery and ultracapacitor cells are typically on the order of 2.3~2.8 V/cell nominal, approximately 92 cells in series were needed (92 cells x 2.4V/cell derated= $\sim$ 221V). This cuts down the total BoostCap "Ceq" in turn that should be modeled according to the equation:

$$(3.1) \quad 1/C_{eq} = 1/C_1 + 1/C_2 + \dots \quad \{\text{BoostCap equivalent Capacitance}\}$$

The total Ceq was found to be  $\sim$ 33F. With the equivalent series resistance (esr) given for a typical 3,000 F cell of 0.29 mohms (Reference 2), the total esr would be (including a 1.3 packaging factor) 34.68mohms (or 0.29 mohms\*92\*1.3). This is the value of esr included with the BoostCap for the simulation. For other values of capacitance a total of 92 cells in series was again used to reach the nominal system voltage with the corresponding combined esr adjusted and Ceq again calculated as above. The corresponding values of capacitance (in F) used from the Maxwell data were subsequently as follows (with Ceq recomputed):

❖ 2000, 1500, 1200, 650, 350

For the remaining values of capacitance (Ceq = 0.111F and 0.005F) a Vishay Aluminum Electrolytic 25V 101/102 PHR-ST 1F and 0.047F cells were used with an esr of 5 mohms and 12 mohms for comparison (Reference 4). In this case, the total esr was calculated as 58.5 mohms and 140.4 mohms respectively (9 cells\*5 mohm\*1.3 and 9 cells\*12 mohm\*1.3) for a nominal initial capacitor voltage of 225V.

A second data series (series #2) was then simulated assuming a 20% reduction in esr per cell could be achieved in each of the cases above. As shown, a moderate but not highly noticeable

improvement is seen (3-10V battery voltage sag improvement in the range of 3.8-30F BoostCap added).

A final data series (series #3) was simulated assuming cold temperature (i.e. less than 0 degrees Celsius) operation. In performing this simulation, a 2x nominal room temperature internal resistance was assumed for the Nickel Metal Hydride Battery (0.6 ohms or 2x0.3 ohms) and a 1.3x nominal room temperature internal resistance was assumed for the BoostCap.

Table 3-1 below provides a complete summary of the equivalent series resistance (Req) calculated for each of the Ceq cases evaluated above during the simulation. The corresponding individual cell resistances are included (Rcell) and, finally, the associated values for the 20% esr reduction and cold temperature series #2 and #3 are included.

Table 3-1: Boost Capacitance characteristics for Simulation

	Ccell (F)	Ceq (F)	Weight (lbs.)	Series #1		Series #2		Series #3	
				Nominal Temperature		20% Rcell reduction		< 0 deg. C Temperature	
			Rcell (mohms)	Req (mohms) (4)	Rcell (mohms) 0.8x nominal	Req (mohms) (4)	Rcell (mohms) 1.3x nominal	Req (mohms) (4)	
	3000	32.6	103	0.29	34.68	0.232	27.75	0.38	45.1
	2000	21.7	73	0.35	41.86	0.28	33.49	0.45	54.4
	1500	16.3	57	0.47	56.2	0.37	44.97	0.61	73.1
	1200	13.0	53	0.58	69.4	0.46	55.49	0.75	90.2
	650	7.1	32	0.80	95.68	0.64	76.54	1.04	124.4
	350	3.8	13	3.2	382.72	2.56	306.17	4.16	497.5
	1	0.111(3)		5	58.5	4.0	46.8	6.5	76.05
	0.047	0.005(3)		12	140.4	9.60	112.32	15.6	182.52

Notes:

- (1) Assumes 92 ultracapacitor cells in series
- (2) Battery internal resistance 0.3 ohms (nominal temperature condition) assumed for Series #1 and #2 and 0.6 ohms (< 0 deg. C temperature condition) assumed for Series #3
- (3) Assumes 9 electrolytic cells in series
- (4) Includes 1.3 assumed packaging factor

The final results are presented below.

### 3.1.2 Simulation Results

It was observed that adding BoostCap in parallel with the battery dramatically improves the amount of voltage “sag” seen at the battery terminals on initial start-up of the DC Motor. For the initial 33F BoostCap case, for example, a 62V improvement is seen in comparison to the case with no additional capacitance (~148V at the battery terminal compared to 210V). It was also noted parallel capacitance must go well below 1F (0.005F) before there are only minimal or no benefits observed. Further, a moderate BoostCap of only 1F proves to be an added benefit in this case. It was also interesting to note reducing the BoostCap equivalent series resistance (esr) by 20% only minimally improves the amount of voltage boost that can be provided on start-up. The dip in the Battery voltage minimum around 5F may be due to the BoostCap becoming a resonant load in this range. In examining this aspect further, it was seen that in applying a 238V step load to the circuit, a linear di/dt current rate rise of 80-amperes per 0.01 sec was seen in series at the battery output. Equating this to inductance results in 29.75mH (from  $V=L \cdot di/dt$ ) that must be present in the circuit including all effects. 3.8F of BoostCap was reconfirmed upon simulations as resulting in the most voltage dip or a frequency resonance point of  $f = 0.473\text{Hz}$  (from  $\omega=1/\sqrt{LC}$  and  $\omega = 2\pi f$ ).

The time for the motor to reach its peak speed was noted as approximately 0.23-0.24 seconds in virtually all of the test runs. For the cold temperature conditions and BoostCap less than 0.111F (including the case without BoostCap) the time for the motor to reach its peak speed was noted as moderately higher (0.3 seconds) with a sag before reaching its maximum.

A summary of the simulation results is provided in figure 3-2 and figure 3-3 and Table 3-2 below.

Table 3-2: Battery Assist Simulation Results

With Capacitor esr given as per data sheet				With improved Capacitor esr by 20%			
Boost Cap (Farad)	Battery min (V)	time to peak Motor speed (sec)	Peak Battery Current (amps)	Boost Cap (Farad)	Battery min (V)	time to peak Motor speed (sec)	
30	210.6	0.23	86	30	212.5	0.23	80
21.74	208.8	0.24	92	21.74	211	0.24	85
16.3	205.5	0.24	104	16.3	208	0.24	95
13.04	202.6	0.24	113	13.04	205.6	0.24	103
7.06	197.7	0.24	129	7.06	201.1	0.24	118
3.8	172.6	0.22	212	3.8	176.5	0.24	200
0.111	187.5	0.23	162	0.111	188	0.24	161
0.005	171.5	0.23	216	0.005	144.5	0.24	305
				Without Boost Capacitor			
				145.5			300
				145.5			300

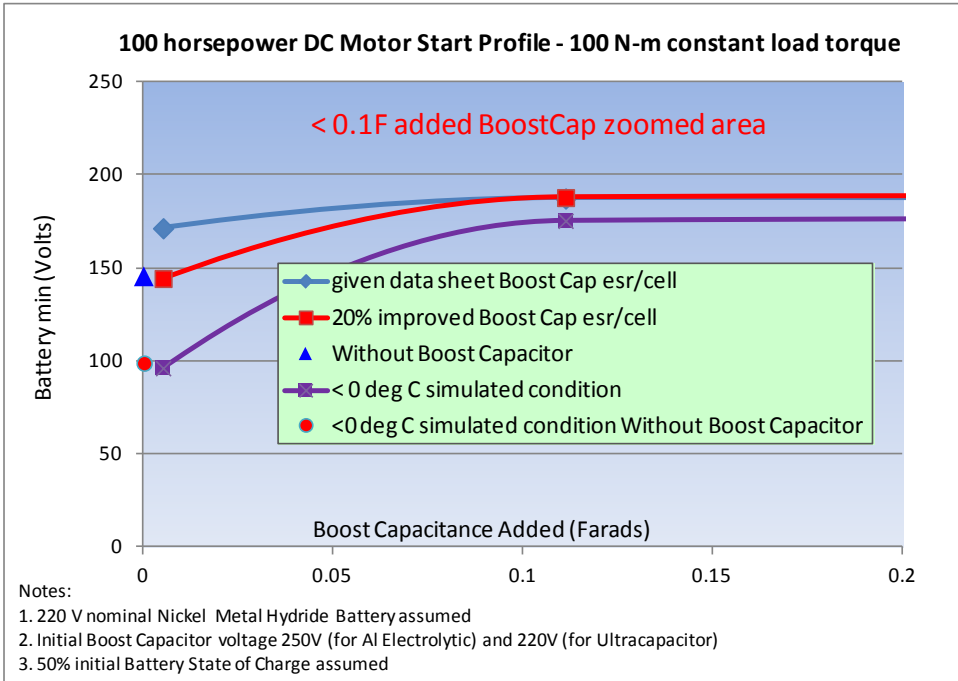
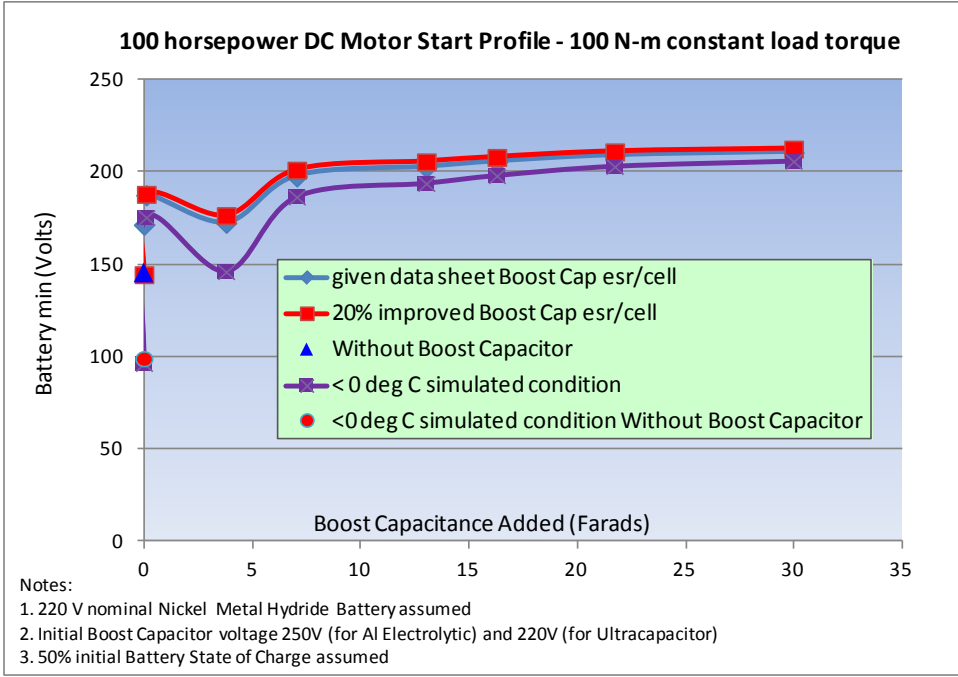


Figure 3-2: Simulation Results (Battery Voltage)

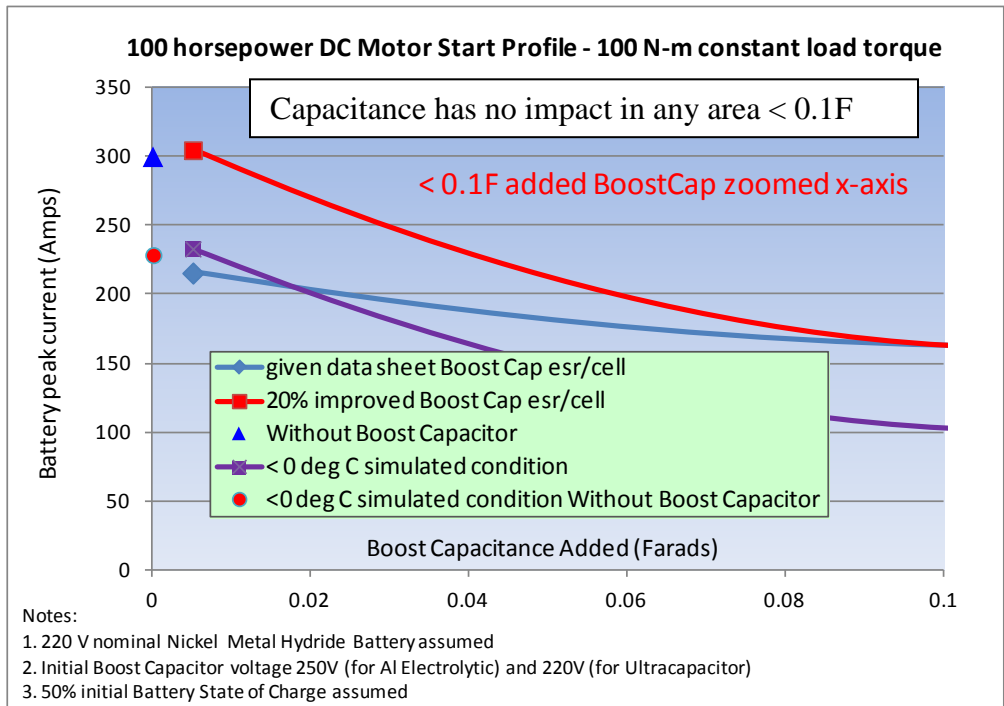
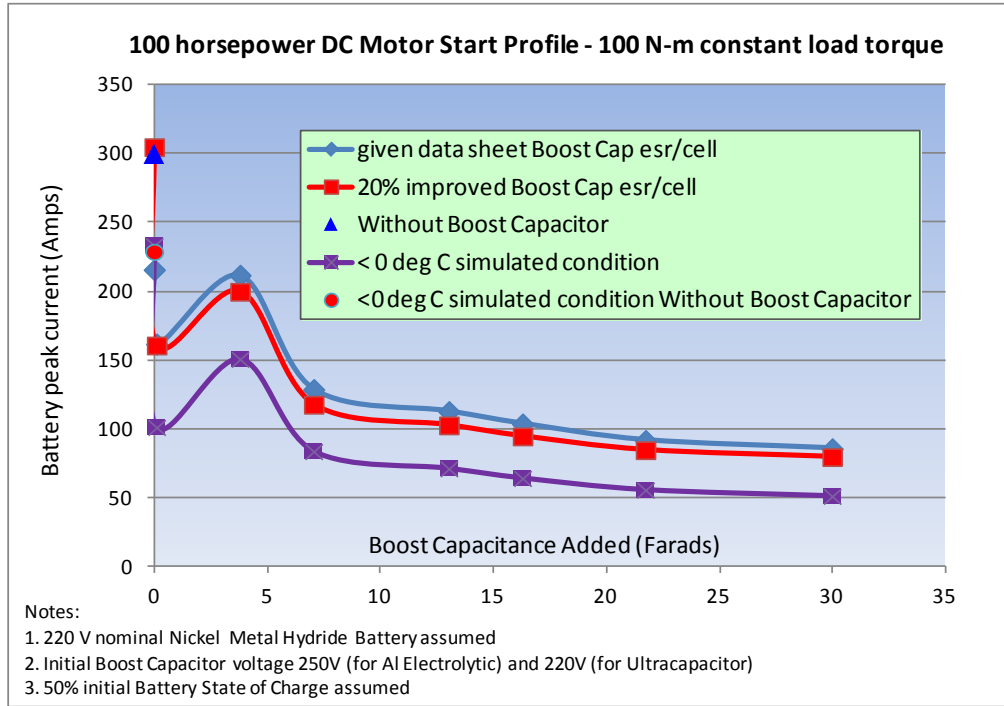


Figure 3-3: Simulation Results (Battery Peak Current)



### 3.1.3 Simulation Conclusion

It was clearly shown how adding capacitance typically attainable from ultracapacitors reduces battery peak current (levels below 130-amps with 7 Farads of BoostCap) and may benefit overall battery operating life as indicated in figure 3-3 above and specifically for highly repetitive APU starting (pending further study – see Follow-On Study Section). Improvements in battery voltage “sag” were also evident and may benefit applications with longer power feeder runs from the APU Starter to the Battery (larger line losses) and would have even a more pronounced improvement in cold temperature conditions. As expected, the amount of “sag” without any BoostCap is much higher at simulated cold temperature conditions than at nominal temperature conditions (150V versus 100V). Values of capacitance typical of ceramic, film or hybrid tantalum capacitors would likely not have benefit in this application due to their limited energy contribution, even within the < 1 second time range, although conceivably many parallel strings could be added for potential benefit at a larger weight penalty.

Finally, trading various nominal system bus voltage levels would be worthwhile for the various approaches and would likely favor ultracapacitors for lower voltage systems versus higher voltage systems. One such attempt at a design study is provided in table 3-3 below where it can be seen there is a higher proportionate amount of weight in higher voltage systems (220V) for an ultracapacitor approach compared to a traditional capacitor design solution vs. a 28V system. Both systems have assumed an equivalent overall capacitance requirement of 1 Farad similar to that derived in the case study. Additionally, it can be seen in both systems the ultracapacitor design is “capacitance oversized” although its overall weight is indeed smaller than a more conventional capacitor solution for both systems.

Table 3-3: System Voltage Comparisons for Battery Start Assist  
220V System – 1 Farad Requirement

Design Solution	Total Weight (lbs.)	Comments
Maxwell 63F Modules, 125V rated (BMOD0063)	269	Assumes two modules in series for total Ceq=31F
Vishay PHR-ST Series 3300 µF cells, 100V rated Aluminum Electrolytic	451	Assumes 909 parallel branches, 3 capacitors in each branch to achieve 1 Farad

**Ultracap solution 0.596x the weight of Al Electrolytic Solution BUT 31x Capacitance needed**

Table 3-3 (Cont.): System Voltage Comparisons for Battery Start Assist  
 28V System – 1 Farad Requirement

Design Solution	Total Weight (lbs.)	Comments
Maxwell 58F Modules, 16V rated (BMOD0058)	2.78	Assumes two modules in series for total $C_{eq}=29F$
Vishay Wet Tantalum 200D Series 2400 $\mu$ F cells, 30V rated	115	Assumes 417 parallel branches, 1 capacitor in each branch to achieve 1 Farad

**Ultracap solution 0.024x the weight of Wet Tantalum Solution BUT 29x Capacitance needed**

A more complete study would be required to assess the weight and efficiency impacts and trade the various approaches for other voltages that might be worthy of consideration (see Follow-On Study Section).

In summary, the following highlights the findings of the Simulation:

- ❖ Improving BoostCap esr has minimal impact for this case study
- ❖ Added BoostCap of 1F or more provides needed improvement
- ❖ Added BoostCap greater than 5F reaches a point of diminishing return

### 3.1.4 Lab Demonstration

In an effort to perform a simple demonstration illustrating the potential benefit of ultracapacitors wired directly in parallel with a battery, a single lithium ion supercapacitor (discussed in Chapter 2 section 2.3) 3,000F cell sample was used in combination with two Nickel Cadmium (NiCad) battery cells placed in series. The LIC cell was provided courtesy of JSR Micro and the battery cells were spares available from the Lockheed Martin Aeronautics Flight Line (C-5 Galaxy Modernization configuration) in Marietta Georgia. A photograph of the LIC cell on the test bench is provided in figure 3-4 below.



Figure 3-4: Lithium Ion Supercapacitor Test Cell

Since the nominal NiCad per cell voltage is approximately 1.2V, it was projected two in series would be required to match the nominal voltage of a single LIC cell (3.8V maximum) assuming a partially discharged state. The intent of the test setup was to evenly match voltage of the two NiCad cells in series to that of the single LIC cell to prevent current “bleeding” from one device into the other just prior to application of the load. In a more typical system design, control electronics could be implemented to perform this function more dynamically and precisely but was outside the scope of this simple demonstration.

Prior to applying the load the voltage on the LIC cell was noted as approximately 3.0V upon measurement (with an oscilloscope) indicating the cell was in a partial state of charge after being stored in the lab for approximately 3 months. The LIC cell was then charged with a constant voltage, constant current power supply to 3.7V and then allowed to discharge to approximately 2.65V. Similarly, the two NiCad cells were charged per the normal NiCad charging procedures and allowed to discharge to approximately 1.325V each (or 2.65V assuming two cells in series).

Finally, the two NiCad cells were then loaded with a 0.5 ohm resistance and the voltage “sag” recorded through an “AC coupled” scope measurement. Just after this initial loading test, the NiCad cells were noted as being relatively unaffected in terms of their overall nominal voltage level and so the testing proceeded by placing the LIC partially discharged cell in parallel with the NiCad cells. The system (NiCad + LIC) was then again loaded with the same 0.5 ohm resistance load and voltage “sag” off the battery recorded (again” AC coupled” measurement). The before and after scope photographs are provided in figure 3-5 below.

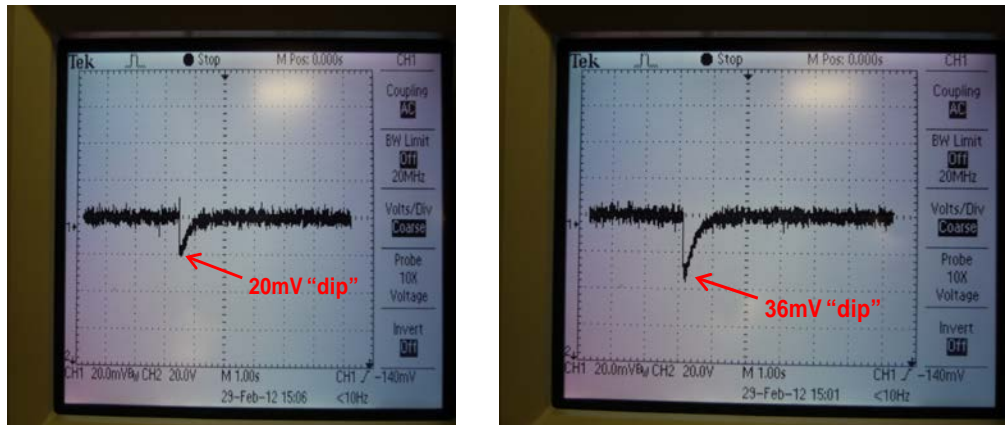


Figure 3-5: Battery voltage “sag” tests (Before and after LIC in parallel)

As can be seen a nearly 45% improvement in voltage “sag” is shown based on this simple demonstration  $((36-20)\text{mV}/36\text{mV})=0.444$ . The demonstration clearly indicates some benefit is provided as the initial voltage (or surface charge) under load is extracted off the ultracapacitor with its lower series resistance (as compared to the battery chemistry). Larger scale demonstrations may also provide similar results and might be used to extrapolate improved battery life projections.

### 3.1.5 Technology Roadmap for Ultracapacitor as Electric-Start Assist Device

Given that improvements were seen in the ability of ultracapacitor technology to improve battery voltage sag in motor electric-start assisting, no significant technology roadmap initiative is deemed to be of high immediate value at this time especially for lower voltage (28V) aircraft systems. Follow on discussion might focus on additional improvements to the start-assist application in ultracapacitor design by quantifying the amount of lengthened battery life due to the observations recorded in this section as well as the other follow-on activity discussed in Chapter 4.1.

## 3.2 Application Study #2 – Peak Load Assist with Capacitance

### 3.2.1 Overview

A second application relates to maintaining a distribution bus at a minimum voltage which is connected to a primary power supply (aircraft engine driven generator) in a large constant power step load condition. In this case, the minimum voltage to be maintained is dictated by military aircraft power quality standards and rigidly defined (in contrast to Application Study #1) to mitigate a “brown-out” condition of the other equipment connected to the common bus with the applied step load. The

momentary, minimum voltage allowable is typically specified as 240V for a nominal 270V system. Momentary step loads of 1.5x (or possibly more) the steady-state rating of the engine generator are possible in future systems.

### 3.2.2 Simulation

LT Spice Version IV was used as the demonstration tool to explore the potential benefits of high levels of capacitance in parallel with a primary 270V supply as a voltage assist scheme. The circuit diagram from LT Spice used for the simulation is shown in figure 3-6 below.

As shown in the simulation diagram, the 270V supply has been represented by a series of inductance and resistive components with the power line to the distribution bus defined as a series R-L circuit representative of 50 ft. of 2 gage wire (Reference 14 MIL-W-22759 wiring specification 0.17 ohms/1000 ft.) and 10μH of line inductance.

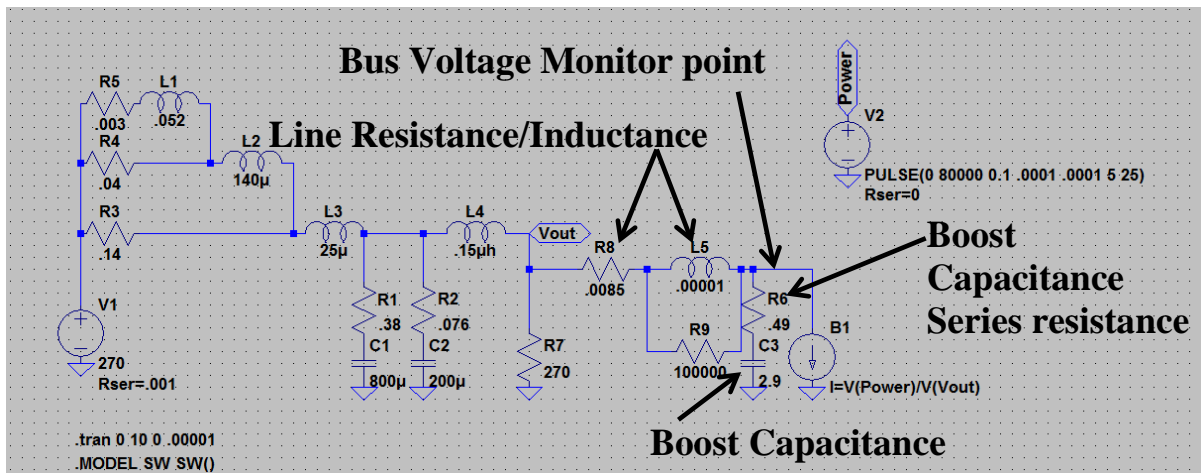


Figure 3-6: Peak Load Buffering LT Spice IV Simulation Circuit

The C3 capacitance represents the varying value of Boost Capacitance. Initially, the value of C3 was set at 30μF as a baseline for comparison with the 80kW constant power, 5 second step load applied at 100 milli-seconds into the simulation. As seen in figure 3-7 below, the voltage sag resulting at the Bus voltage Monitor point is 189V (well below the 240V minimum allowable).

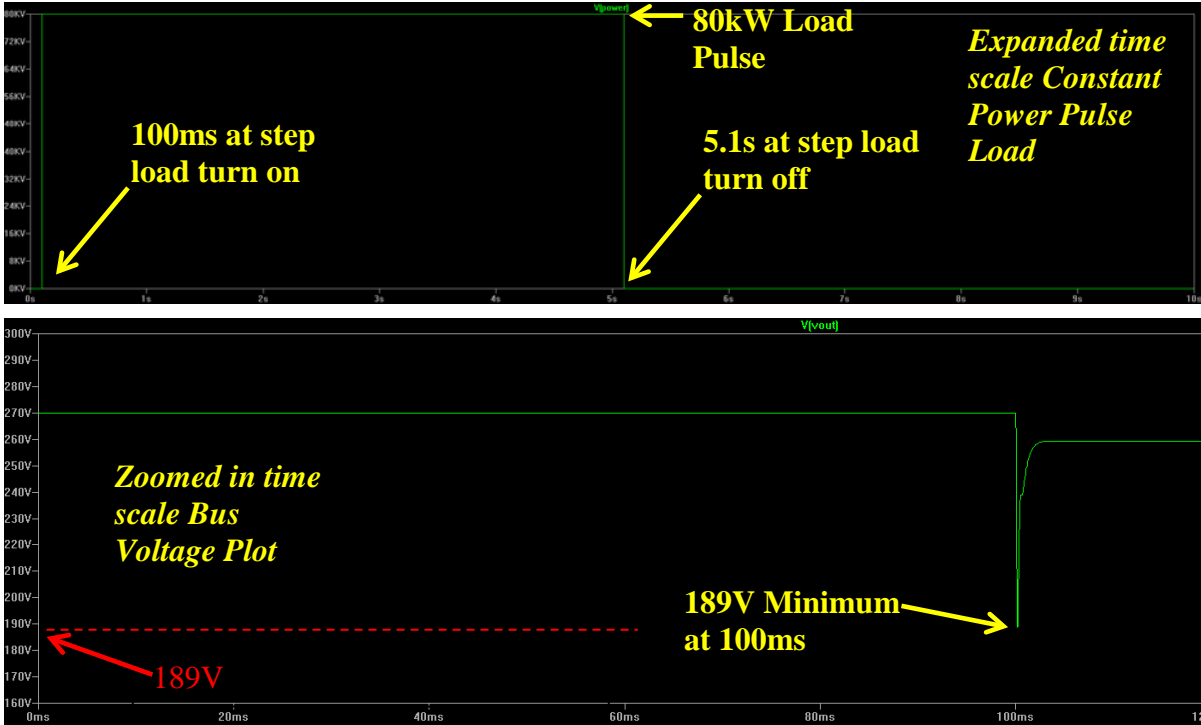


Figure 3-7: LT Spice IV Simulation Results - 30  $\mu$ F Low Boost Capacitance with Constant Power Load

In expanding the study, two representative 160V, 5.8F Maxwell Ultracapacitor modules (ref: <http://www.maxwell.com/products/ultracapacitors/160v-module>) in series were used as the C3 element and the voltage sag was observed as improving to 208V minimum (but again below the minimum 240V allowable) as shown in figure 3-8 below. Regenerative Energy “Bounce-back”, as expected, is also observed when the load is removed. 0.49 ohms was used as the boost capacitance series resistance of the modules and derived by:

$$240\text{m}\Omega \text{ (specification resistance per module)} \times 2 \text{ modules in series} = 480\text{m}\Omega + 10\text{m}\Omega^{**} = 0.49\Omega$$

\*\* additional resistance approximation due to interconnects as provided by Maxwell Applications Engineering

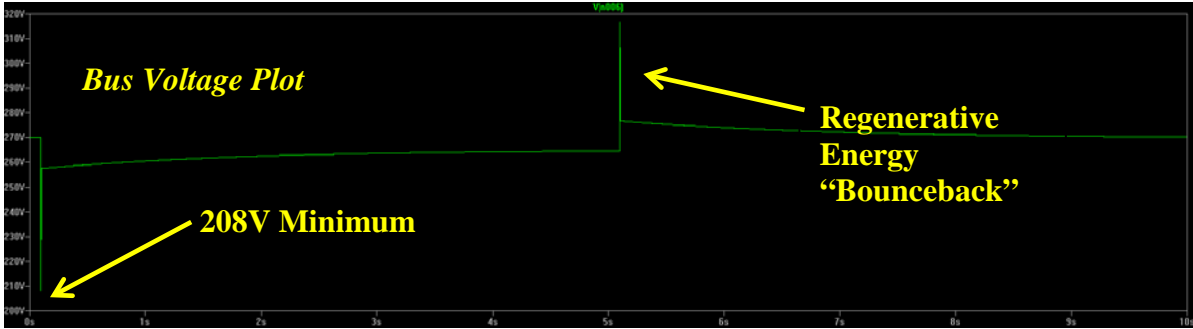


Figure 3-8: LT Spice IV Simulation Results – 2.9F Boost Capacitance with Constant Power Load

Finally, varying the amount of boost capacitance series resistance (and assuming the 2.9F could be maintained) gave the following results:

Boost Capacitance = 2.9F

<u>Boost Cap Resistance (<math>\Omega</math>)</u>	<u>Bus Voltage Sag (V)</u>
0.49	208
0.29	222
0.19	233
<b>0.15</b>	<b>240 &lt; Target Voltage minimum</b>

With 120 cells in series (or two 160V modules in series, 60 cells each at 350F per cell) this means that (not including the additional interconnect resistance as is included in the above summary) 140m $\Omega$  total must be achieved or nearly a 70% reduction from the Maxwell specification value of 480m $\Omega$ .

### 3.2.3 Simulation Conclusion

The results of the LT Spice simulation for the Peak Load Assist case highlights:

- ❖ >50% improvements in ultracapacitor cell esr is needed to maintain minimum bus voltage requirements
- ❖ Expansion of ultracapacitor energy density is of minimal added value in this case

Of course, capacitor modules can always be paralleled to reduce the total Req and attack bullet 1 above but at a potentially unacceptable weight penalty to the system design for tactical, weight sensitive platforms.

### 3.2.4 Lab Testing

A simple test was executed to assess the actual performance of ultracapacitor technology as a boost element in parallel with a power supply. For the lab test, a 16V, 110 F (nameplate) Maxwell ultracapacitor module was used which had been stored in office space for approximately four years.

The intent of the test was to perform scaled down (i.e. scaled down loading) testing using actual hardware with available test equipment in the Lockheed Martin Fort Worth power lab. A 16V power supply was identified as optimal for the test and matched the ultracapacitor module rating. Figure 3-9 below provides the initial notional sketch of the test layout.

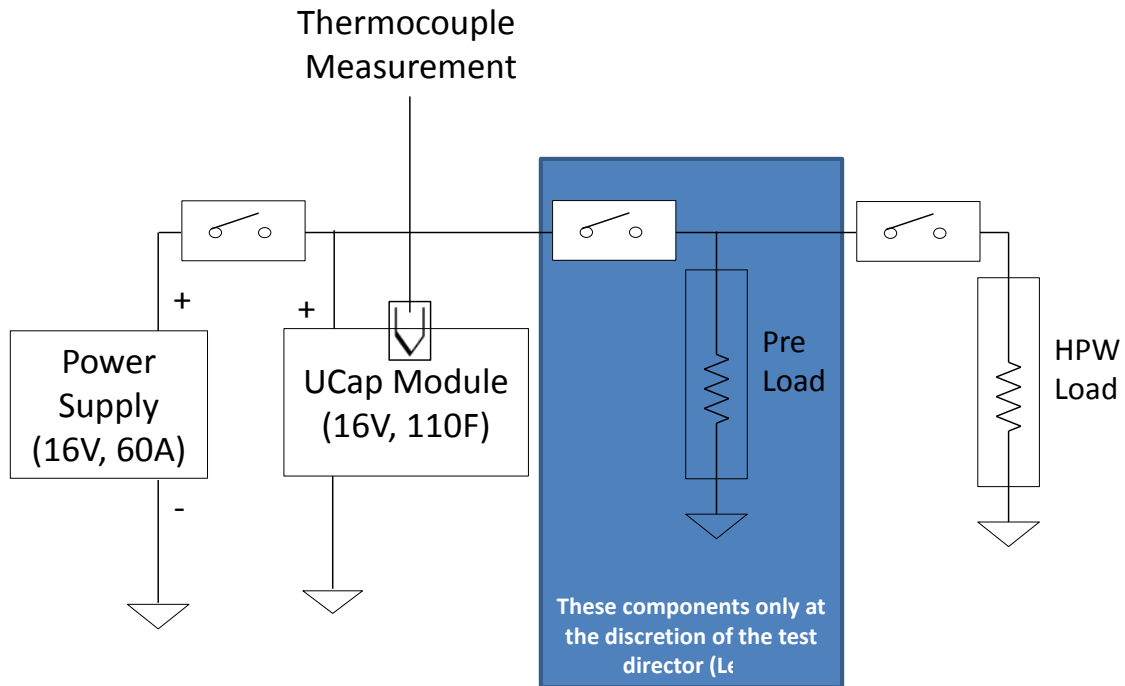


Figure 3-9: Step Load Initial Test Layout Concept

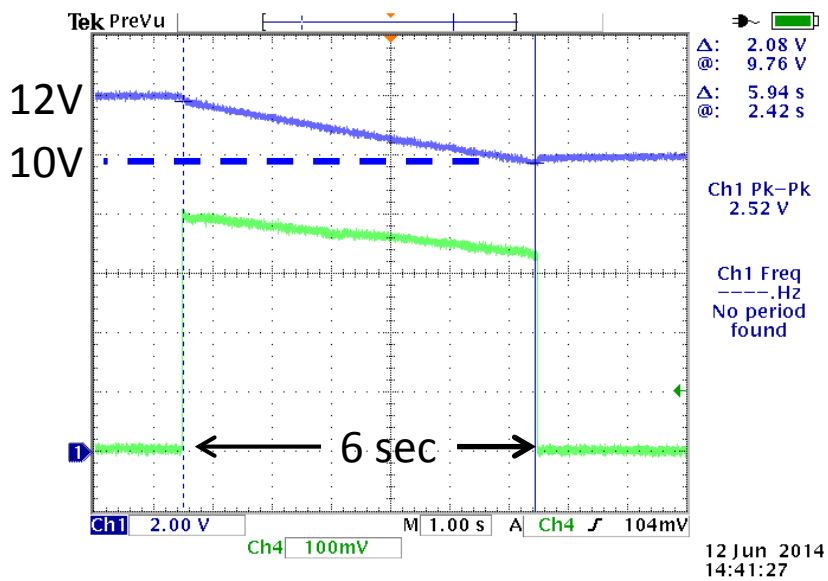
The initial testing performed was intended to evaluate the actual state of the module. By applying a 1-amp charge to the module an unusually high charge time was noted (based on  $C \cdot \Delta v / \Delta t$ ). Subsequent inspection determined external sensor jumpers were shorted together and then corrected by disconnecting them.

Upon reapplying 1-amp from the power supply the expected charge time was observed based on:



(3.2):  $I=C*(\Delta v/\Delta t) \rightarrow 1\text{-amp} = 110\text{F}*(\Delta v/\Delta t) \rightarrow (\Delta v/\Delta t) = 1/110$  or: 0.009 V/sec or 22 minutes to charge up to 12V. Note the module was not taken up to the full 16V rating. This measurement validated the 110F rating of the module.

Upon charging up to 12V the module was then discharged into a 0.3Ω (or 40-amps) very small duration step load with no noticeable initial voltage sag. Subsequent 3-6 second duration 40-amp step loads were applied with 10-12V gradual decay observed from the ultracapacitor module with the results shown in figure 3-10 below.



## 12-10V Voltage Decay

Figure 3-10: Step Load Testing with 40-amp load

Finally, test loading applied was increased to 200-amps by utilizing a spool of 8 awg wire trimmed down to a size to yield 60mΩ measured with an ohmmeter and thus:

$$\diamond 12/0.06 = 200\text{-amps}$$

In these conditions, large initial voltage sag was noted (approximately 20% of the initial voltage). The results are provided in figure 3-11 below.

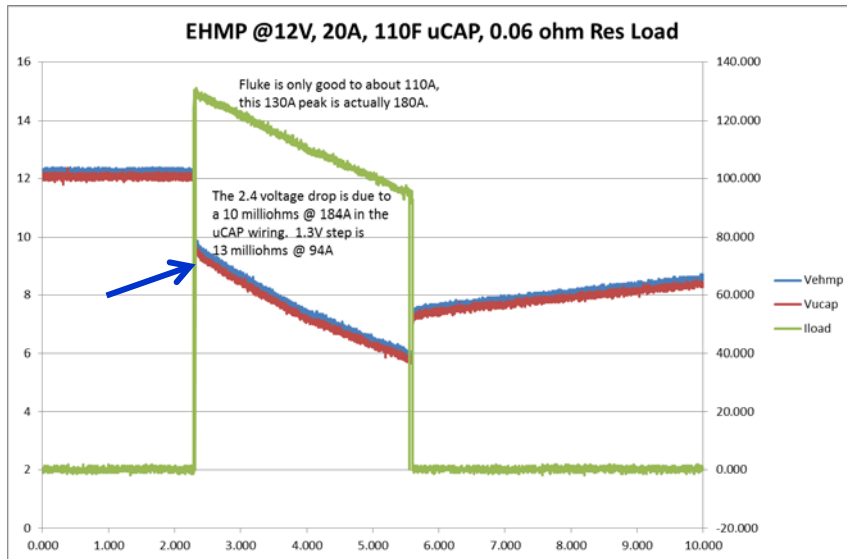


Figure 3-11: Step Load Testing with 200-amp load

This voltage sag was initially thought to be due to the wiring of the test set up but upon further investigation was found to be due to the specified increase in the ultracapacitor module series resistance over time. Per the “Life” Section of a typical 16V module datasheet (ref: [http://www.maxwell.com/products/ultracapacitors/docs/datasheet\\_16v\\_small\\_cell\\_module.pdf](http://www.maxwell.com/products/ultracapacitors/docs/datasheet_16v_small_cell_module.pdf)):

- ❖ “ESR Change (% increase from maximum initial value): 100%”

### 3.2.5 Technology Roadmap for Peak Load Assist - Ultracap as a Baseline

A technology roadmap outline discussion based on the observations in this section can be summarized in that:

- ❖ Improvements in ultracapacitor cell resistance are required to meet high step load conditions where a minimum voltage must be maintained at a bus
- ❖ Improvements must be made in the storage life cell resistance rise of ultracapacitors


Again, paralleling multiple ultracapacitor modules may not be an option in some weight sensitive applications. This can be seen, for example, in assuming four parallel strings are modified to the case studied in Chapter 3.2.2 to achieve the required reduction in resistance, or:

$$0.49\Omega // 0.49\Omega // 0.49\Omega // 0.49\Omega = 0.1225\Omega$$

Given each 160V module weighs 5.2kg (per the Maxwell data sheet) or approximately 11.46 lbs., the total weight (not including required interconnects, etc.) of the unmodified Chapter 3.2.2 configuration is 22.92 lbs. In the assumed configuration with four parallel sets of two 160V modules in series the total weight is increased to 4\*22.92 lbs. or 91.68 lbs. This equates to an approximate weight growth of 70 lbs. (4x) and not uncommon for a hardware candidate to be disqualified entirely for further consideration unless substantial reliability improvements can be demonstrated.

In examining various ultracapacitor devices available on the market, the following table (taken from Reference 9) does indicate Yunasko technology shows a nearly 44% improvement over the Maxwell technology in cell resistance and may be a better candidate for future study.

Table 3-4: Ultracapacitor Technology Resistance Comparisons

	Capacitance <sup>#</sup> (F)	DC Resistance <sup>*</sup> ( $\mu\Omega$ )	 ESR ( $\mu\Omega$ )	Stored Energy <sup>#</sup> (Wh/kg)	Response Time <sup>^</sup> (s)
Maxwell	3140 +/- 16	230 +/- 15	162	4.5	0.7
Ioxus	3100 +/-34	230 +/- 21	174	4.3	0.7
NCC	1090 +/- 22	860 +/- 26	420	2.8	1.1
Yunasko	1230 +/- 14	160 +/- 45	92	4.0	0.2
JM Energy	1090 +/- 2.3	2100 +/- 72	990	10	2.3
Batscap	1290 +/- 5.7	330 +/- 45	240	4.0	0.4

\* The tolerances listed are one standard deviation of the twelve cells measured  
 # Calculated assuming discharge to half rated voltage except JM Energy full voltage window  
 ^ Calculated as product of the DC resistance and rated capacitance

## Chapter 4: Summary

This paper has examined various energy storage evolving technologies and their potential application to aircraft. Although neither the lab nor simulation demonstrations were intended to be an all exhaustive study including the many various effects mentioned, they do illustrate general principles in the utility of ultracapacitor technology to evolving aircraft applications. The results of the two case studies have clearly shown how two different applications drive different needs in ultracapacitor technology.

In the case of boost capacitance to boost a battery supply to start a motor (and specifically applied to the cold temperature conditions) off-the-shelf technology is well suited to aid the battery supply. In these cases, the minimum voltage to the starter motor is allowed to sag an appreciable, momentary amount to turn the motor with any amount of peak battery current decrease deemed of value although it was seen how lower ultracapacitor cell voltage drives higher weight for higher voltage systems. This research has also shown in the case studied related to large, constant power pulse loading that many existing off-the-shelf ultracapacitor technologies may not possess low enough series resistance to maintain required minimum voltages at the bus without additional paralleling. Furthermore, the additional paralleling of devices to reduce equivalent resistance may not be acceptable in weight sensitive platforms. Additional capacitance provided minimal value in this case.

Many other exciting forms of energy storage technology advances (as referenced in the Ragone plot) were not explored in detail within this paper but details can be found by the curious reader. Such concepts vary from both the package to material study and device physics levels, vary widely in technology maturity and are constantly evolving/changing.

These technologies, in summary, include:

- ❖ Magnetic Capacitors
- ❖ Supercapacitor electrolyte improvements
- ❖ Antiferroelectric and ceramic material development
- ❖ Nanomaterials and nanotube (aligned) structures
- ❖ Graphene based supercapacitors
- ❖ Lithium-Air Batteries
- ❖ Zinc-Air Batteries
- ❖ Thermal Battery (non-rechargeable) enhancements
- ❖ Flywheels
- ❖ Lithium Ion Battery power density (packaging) improvements

All the above observations can be used in forming an “Investment Strategy” proposal. Table 4-1 outlines key technologies with an existing usage, near and far term focus. It is left to curious investigators of technologies to fill in the unknown areas, disagree or add.

Table 4-1: Energy Storage Investment Strategy Proposal

Realm	Current Power Source	Near-term	Far-term
Munitions	Squibbed Thermal Battery	Zinc-Air	High-voltage diamond Ultracapacitor
Aircraft	Lithium Ion	Improved power dense UltraCaps, High power variant Lithium Ion	Magnetic Capacitor
Satellite	Nickel-Hydrogen Battery	??	??
Automobile	Lithium Ion, Ultracaps	??	??

Finally, relating this activity to non-aircraft applications such as the DC Micro-Grid, it can be seen in observing sample papers (Reference 10 taken from the internet site: [http://der.lbl.gov/sites/der.lbl.gov/files/lse\\_2010.pdf](http://der.lbl.gov/sites/der.lbl.gov/files/lse_2010.pdf)) that ultracapacitors are viewed as a potential energy storage technology on the output side of the distribution system grid AC:DC (6kV:200V) Transformer. In this instance, ultracapacitors are shown in tandem with both a battery and gas engine cogeneration system to supplement the grid supply and improve power quality to a Photovoltaic System and other downstream DC:AC Inverters for residential power. Reference 15 also discusses the utilization of ultracapacitors in two different electric grid configurations. Figure 1-4 as shown previously also provides a notional hybrid vehicle system where ultracapacitors might replace the battery as the energy storage supply.

#### 4.1 Follow-On Activity

The following items are captured from this research as follow-on with some portion of them perhaps eventually related to PhD pursuits:

- 1) Quantify any amount of lengthened battery life due to Ultracapacitor in parallel with Battery Case over typical aircraft operating life
- 2) Characterize how stiffer buses created with energy storage supplies might improve the engine generator design (improve life)
- 3) Further characterize cold temperature BoostCap resistance fidelity for simulations
- 4) Further examine high frequency ripple current impacts on ultracapacitors (operating life, etc.)
- 5) Examine how more detailed non-linear models of ultracapacitors (voltage dependent effects) might be implemented in the circuit simulations

Contact Information:

Roger Brewer, [roger.brewer@lmco.com](mailto:roger.brewer@lmco.com), Lockheed Martin Aeronautical Systems, Ft Worth, TX Tele:  
817-762-2482

## References

- (1) Handbook of Batteries and Fuel Cells by David Linden, 1984
- (2) Maxwell Technology comparison
- (3) 2011 21<sup>st</sup> International Seminar on Double Layer Capacitors and Hybrid Energy Storage Devices  
(<http://www.supercapseminar.com/>)
- (4) Vishay Aluminum Electrolytic 101/102 PHR-ST Series data sheet
- (5) Maxwell Technologies 2005 Product Guide
- (6) Paper presented by Dr. John R. Miller at 2011 21<sup>st</sup> International Seminar on Double Layer Capacitors and Hybrid Energy Storage Devices “Electrochemical Capacitor Performance Metrics”
- (7) Electrical-Energy-Storage Unit (EESU) US Patent 7,033,406 B2
- (8) MAE/ECE 535 Design of Electromechanical Systems Class Notes Spring 2012, Section II  
Fundamentals of Electromagnetism
- (9) “Life Performance of Large Electrochemical Capacitors” by John R. Miller, Sue M. Butler and Seana McNeal
- (10) “DC MicroGrids and Distribution Systems for Residences” by Toshifumi ISE, Hiroaki KAKIGANO, Osaka University, JAPAN
- (11) “Comparison of ultracapacitor electric circuit models” by Lisheng Shi ;Electrical and Computer Engineering Department., Univ. of Missouri-Rolla, Rolla, MO
- (12) “Fractional-order models of the supercapacitors in the form of RC ladder networks” by W. Mitkowski and P. Skruch, Faculty of Electrical Engineering, Automatics, Computer Science and Biomedical Engineering, Department of Automatics and Biomedical Engineering, AGH University of Science and Technology, 30/B1 A. Mickiewicza Ave., 30-059 Cracow, Poland
- (13) “Electrochemical Capacitor Characterization for Electric Utility Applications” by Stanley Atcitty, Dissertation submitted to the faculty of the Virginia Polytechnic Institute and State University in partial fulfillment of the requirements for the degree of Doctor of Philosophy in Electrical Engineering

## **References (Cont.)**

(14) Military Wiring Specification MIL-W-22759/1F 18 September 1992

(15) "Characteristics of Electrochemical Capacitors for Electric Utility Applications" by Stanley Atcitty



## Appendix

## **Appendix A- Generator Instability in Aircraft Power**

The issue of high peak and low power loads and its impact on primary power shaft driven aircraft generators is becoming an increasing concern, specifically in terms of both the stability and reliability impacts upon the machine. Most military aircraft generators are typically synchronous wound rotor (with the engine rotating shaft as the input or  $P_M$ ) with an excitation field ( $E_{fd}$ ) used for control and regulation of 400 Hertz (Hz) output.

The concept of machine destabilization (bifurcation) under high peak (often well in excess of the machine's steady-state rating or 10x) and very low loads and how energy storage might be used to mitigate the undesirable impacts was initially the target set forth in ECE736 Power System Stability course final project (Spring 2014 semester). However, it was discovered during the simulations that load plays no impact on machine stability that can be directly modelled – only gain K in the controller seems to affect stability.

The focus of the ECE736 project then became targeted at assessing how controller gains modeled impact machine performance. Eventually the impacts of 'beat frequencies' (typically around 10x the nominal aircraft generator frequency (or  $10 \times 400 = 4000$  Hz) that make their way into the control loop (as discussed with a Lockheed Martin colleague and experienced power designer) were assessed. These impacts have been seen in actual military power systems resulting in machine instabilities and the effect was finally successfully modelled by injecting a 4000 Hz signal at the machine  $V_f$  input (found to be the optimal injection point through trial and error) shown in figure A-1. Under the condition modelled, the machine was otherwise at the Controller Output Gain = 9000 and Voltage Controller Gain = -50 condition.

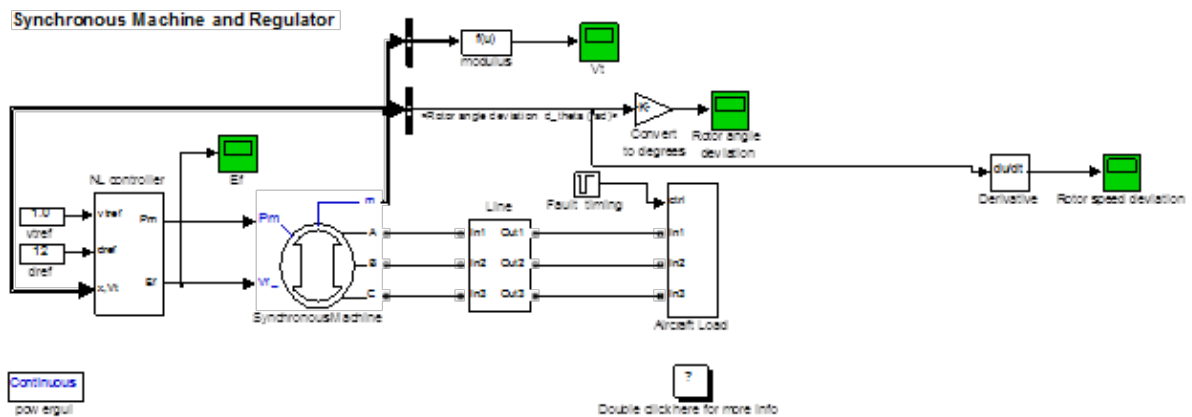


Figure A-1: Generator Stability Study Model

The Synchronous Machine and Aircraft load models were represented as follows:

Synchronous Machine  
Rating: 60kW  
Line-line Voltage:  $120\sqrt{2}V$

Aircraft (Baseline) Load  
Voltage:  $120kV\sqrt{2}V$   
Frequency: 400 Hz

The controller portion was partitioned into two input sections: a) Voltage Controller with gain and b) Speed Controller with gain. This allowed the model gain to be varied in these two aspects and stability observations made.

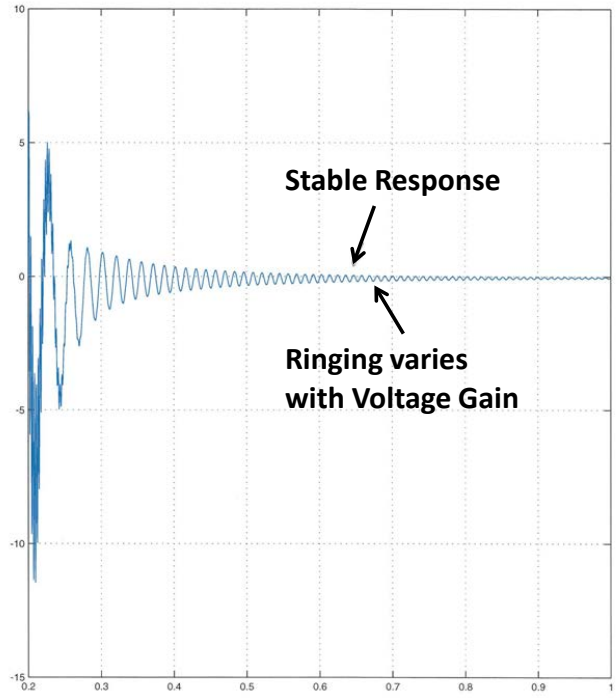
### *Other Initial Observations*

In performing the baseline load run, the system was observed to be stable. A second AC load was then added and varied up to 100kW, then 1MW with no signs of instability noted (indicating stability is not a factor of applied load). The task then became to alter the model and determine first where instability could be noted. It was discovered that by primarily varying the Controller Output Gain K from 1224 to around 1800 and above the system becomes unstable (with Voltage Controller Gain set to -5000). By varying the Voltage Controller Gain down to -7 system stability could be recovered easily for large Controller Gain (5000 and above). Varying the Voltage Controller Gain was also seen as altering the rotor speed deviation response (slightly larger sag noted with large Controller Gain K and higher ringing noted with lower Controller Gain K with Voltage Controller Gain in the -10 to -50 range). Varying the Speed Controller Gain K had little impact on overall machine stability and response.

### *Simulation Results*

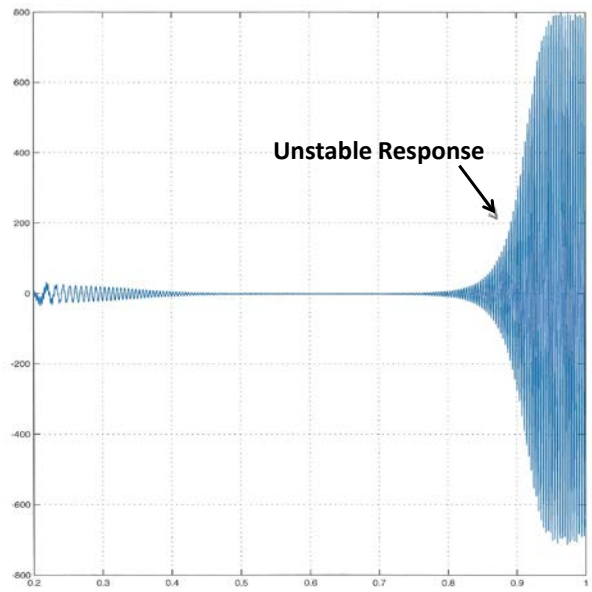
The results from the simulations are provided in figure A-2 below.

Prior to  
Noise  
Injection



Controller  
Output Gain  
= 9,000  
Voltage  
Gain = -50

After Noise  
Injection



Controller  
Output Gain  
= 9,000  
Voltage  
Gain = -50

Figure A-2: Generator Stability Study Results